
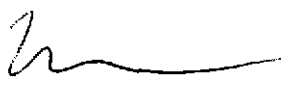


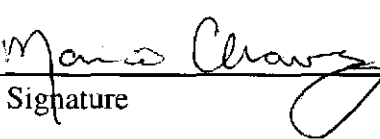
**Sandia National Laboratories
Waste Isolation Pilot Plant**

**Analysis Package for Direct Brine Releases:
Compliance Recertification Application - 2009**

Author: Daniel Clayton (6711)  4/3/08
Print Signature Date

Technical Review: Martin Nemer (6711)  4/3/08
Print Signature Date

Management Review: Moo Lee (6710)  4/3/08
Print Signature Date

QA Review: Mario Chavez (6710)  4/4/08
Print Signature Date

WIPP:1.2.5:PA:QA-L:547488

Information Only

Table of Contents

1	Executive Summary	5
2	Introduction and Background.....	5
3	Background	6
4	Approach.....	9
4.1	Model Geometry	9
4.2	Initial Conditions	11
4.3	Information Specific to the CRA-2009 PA.....	12
4.3.1	Maximum Direct Brine Release Duration	12
4.3.2	Capillary Pressure and Relative Permeability Model	12
4.3.3	Updated Input Parameter Calculation	13
4.3.4	Computer Code Updates	15
4.3.5	Halite/Disturbed Rock Zone Porosity	15
4.3.6	Input File Corrections	15
5	Calculation Methodology.....	16
5.1	Modeled Scenarios.....	16
5.1.1	Scenario 1 (S1).....	16
5.1.2	Scenario 2 (S2).....	17
5.1.3	Scenario 3 (S3).....	17
5.1.4	Scenario 4 (S4).....	17
5.1.5	Scenario 5 (S5).....	18
5.2	Computational Modeling Process.....	18
5.2.1	Grid Generation and Material Assignments.....	18
5.2.2	Initial Conditions, Sampled and Calculated Input Parameters....	18
5.2.3	Calculation of Direct Brine Release Volumes	20
5.2.4	Post-Processing of Results	20
6	Results.....	21
6.1	Summary	21
6.2	Direct Brine Releases from the Lower Drilling Location	22
6.3	Sensitivity of Direct Brine Releases to Input Parameters	36
6.4	Conclusions.....	37
7	Software List.....	42
8	References.....	43

List of Tables

Table 5-1. Intrusion times modeled by DBR for each scenario. 16
Table 6-1. Summary of differences between DBR calculations. 22
Table 6-2. Summary table of number of vectors with non-zero, maximum and average DBR volumes for the S1 DBR calculations. 23
Table 6-3. Summary table of number of vectors with non-zero, maximum and average DBR volumes for the S2 DBR calculations. 24
Table 6-4. Summary table of number of vectors with non-zero, maximum and average DBR volumes for the S3 DBR calculations. 25
Table 6-5. Summary table of number of vectors with non-zero, maximum and average DBR volumes for the S4 DBR calculations. 26
Table 6-6. Summary table of number of vectors with non-zero, maximum and average DBR volumes for the S5 DBR calculations. 27
Table 7-1. Codes that were used in the CRA-2009 PA DBR calculations. 42

List of Figures

Figure 1. CRA-2009 PA DBR material map (logical grid). 10
Figure 2. Regions to be used to transfer initial pressure and saturation between the 10,000 year BRAGFLO grid and the DBR grid for the CRA-2009 PA. 11
Figure 3. Scatter plot of pressure in the disturbed rock zone porosity vs. DBR volumes for the S2 scenario, lower drilling intrusion, CRA-2009 PA. Symbols indicate intrusion times in years. 30
Figure 4. Scatter plot of pressure in the disturbed rock zone porosity vs. DBR volumes for the S2 scenario, lower drilling intrusion, CRA-2004 PABC. Symbols indicate intrusion times in years. 30
Figure 5. Probability plot showing the percentage of the vectors on the X-axis where DBR volumes are less than the value on the Y-axis for the CRA-2009 PA lower drilling location; S1 scenario. 31
Figure 6. Probability plot showing the percentage of the vectors on the X-axis where DBR volumes are less than the value on the Y-axis for the CRA-2004 PABC lower drilling location; S1 scenario. 31
Figure 7. Probability plot showing the percentage of the vectors on the X-axis where DBR volumes are less than the value on the Y-axis for the CRA-2009 PA lower drilling location; S2 scenario. 32
Figure 8. Probability plot showing the percentage of the vectors on the X-axis where DBR volumes are less than the value on the Y-axis for the CRA-2004 PABC lower drilling location; S2 scenario. 32
Figure 9. Probability plot showing the percentage of the vectors on the X-axis where DBR volumes are less than the value on the Y-axis for the CRA-2009 PA lower drilling location; S3 scenario. 33

Figure 10. Probability plot showing the percentage of the vectors on the X-axis where DBR volumes are less than the value on the Y-axis for the CRA-2004 PABC lower drilling location; S3 scenario. 33

Figure 11. Probability plot showing the percentage of the vectors on the X-axis where DBR volumes are less than the value on the Y-axis for the CRA-2009 PA lower drilling location; S4 scenario. 34

Figure 12. Probability plot showing the percentage of the vectors on the X-axis where DBR volumes are less than the value on the Y-axis for the CRA-2004 PABC lower drilling location; S4 scenario. 34

Figure 13. Probability plot showing the percentage of the vectors on the X-axis where DBR volumes are less than the value on the Y-axis for the CRA-2009 PA lower drilling location; S5 scenario. 35

Figure 14. Probability plot showing the percentage of the vectors on the X-axis where DBR volumes are less than the value on the Y-axis for the CRA-2004 PABC lower drilling location; S5 scenario. 35

Figure 15. Scatter plot of pressure in the intruded panel vs. DBR volumes for the S2 scenario, lower drilling intrusion, CRA-2009 PA. Symbols indicate intrusion times in years. 38

Figure 16. Scatter plot of pressure in the intruded panel vs. DBR volumes for the S2 scenario, lower drilling intrusion, CRA-2004 PABC. Symbols indicate intrusion times in years. 38

Figure 17. Scatter plot of pressure in the intruded panel vs. DBR volumes for the S2 scenario, lower drilling intrusion, CRA-2009 PA. Symbols indicate the range of mobile brine saturation. 39

Figure 18. Scatter plot of pressure in the intruded panel vs. DBR volumes for the S2 scenario, lower drilling intrusion, CRA-2004 PABC. Symbols indicate the range of mobile brine saturation. 39

Figure 19. Scatter plot of pressure vs. mobile brine saturation for the S2 scenario, lower drilling intrusion, all intrusion times, CRA-2009 PA. Symbols indicate the range of DBR volumes in m³. 40

Figure 20. Scatter plot of pressure vs. mobile brine saturation for the S2 scenario, lower drilling intrusion, all intrusion times, CRA-2004 PABC. Symbols indicate the range of DBR volumes in m³. 40

Figure 21. Scatter plot of the log of borehole permeability vs. DBR volumes for the S2 scenario, lower drilling intrusion, CRA-2009 PA. Symbols indicate the intrusion time in years. 41

Figure 22. Scatter plot of the log of borehole permeability vs. DBR volumes for the S2 scenario, lower drilling intrusion, CRA-2004 PABC. Symbols indicate the intrusion time in years. 41

1 EXECUTIVE SUMMARY

This report describes and compares the results of direct brine release (DBR) calculations for the CRA-2009 PA to results of the CRA-2004 PABC. Changes to the DBR calculations from the CRA-2004 PABC for the CRA-2009 PA include the reduction of the maximum DBR duration; updated capillary pressure and relative permeability model; updated the parameter calculations for the well productivity index and material permeabilities; incorporation of computer code updates; corrections of the halite and disturbed rock zone porosity values; and corrections of input file errors. These changes will not adversely affect overall releases. While the CRA-2009 PA resulted in an increase in the number of non-zero DBR volumes over the CRA-2004 PABC, the overall maximum DBR volume decreased.

2 INTRODUCTION AND BACKGROUND

The Waste Isolation Pilot Plant (WIPP) is located in southeastern New Mexico and has been developed by the U.S. Department of Energy (DOE) for the geologic (deep underground) disposal of transuranic (TRU) waste (U.S. DOE 1980; U.S. DOE 1990; U.S. DOE 1993). In 1992, Congress designated the U.S. Environmental Protection Agency (EPA) as WIPP's official regulator, and mandated that once DOE demonstrated to EPA's satisfaction that WIPP complied with Title 40 of the Code of Federal Regulations, Part 191 (U.S. DOE 1996; U.S. EPA 1996), EPA would certify the repository. To show compliance with the regulations the DOE had their scientific advisor, Sandia National Laboratories (SNL) develop a computational modeling system to predict the future performance of the repository for 10,000 years after closure. SNL has developed a system called WIPP Performance Assessment (PA), which examines failure scenarios, quantifies their likelihoods, estimates potential releases to the surface or the site boundary, and evaluates the potential consequences, including uncertainties. The regulation also requires that these models be maintained and updated with new information to be part of a recertification process that occurs at five-year intervals after the first waste is received at the site.

In October 1996, DOE submitted the Compliance Certification Application (CCA) to the EPA, which included the results of the WIPP PA system. During the review of the CCA, EPA mandated an additional Performance Assessment Verification Test (PAVT), which revised selected CCA inputs to the PA (SNL 1997). The PAVT analysis ran the full suite of WIPP PA software and confirmed the conclusions of the CCA analysis that the repository design met the regulations. Following the receipt of the PAVT analysis, EPA ruled in May 1997 that WIPP had met the regulations for permanent disposal of transuranic waste. Several lawsuits in opposition to the EPA's ruling were filed in court and were eventually dismissed. The first shipment of radioactive waste from the nation's nuclear weapons complex arrived at the WIPP site in late March 1999, starting the five-year clock for the site's required recertification. The results of CCA PA analyses were subsequently summarized in a SNL report (Helton et al. 1998).

The WIPP Land Withdrawal Act (U.S. Congress 1992) requires DOE to submit documentation to EPA for the recertification of the WIPP every five years following the first receipt of waste in order to continue operations at the site. This documentation in the form of a Compliance Recertification Application (CRA) was prepared and submitted to the EPA by March 26, 2004. This application included an updated PA calculation referred to as the CRA-

2004. The EPA reviewed the application and notified DOE that a revised PA calculation would be necessary in order that the WIPP could be recertified (Cotsworth 2005). This revised calculation is referred to as the 2004 Compliance Recertification Application Performance Assessment Baseline Calculation (CRA-2004 PABC, Leigh et al. 2005). With the EPA's recertification decision in 2006, the CRA-2004 PABC was established as the PA baseline.

Continued review of the CRA-2004 PABC has shown that a number of technical changes and corrections are necessary. Furthermore, updates to parameters and improvements to the PA computer codes have been developed since the CRA-2004 PABC. As the Land Withdrawal Act (U.S. Congress 1992) requires that the DOE apply for recertification every five years from the first receipt of waste, a Compliance Recertification Application is required no later than March 2009 (CRA-2009). Part of the application includes an updated PA calculation referred to as the CRA-2009 PA.

The WIPP PA system consists of a suite of software designed to predict repository performance over a period of 10,000 years. This system includes models which predict conditions (chemical and physical) in the repository over time and consequences of events that might occur in the future. In addition the system evaluates the propagation of uncertainties in both knowledge about the repository (subjective uncertainty) and uncertainty in what might occur in the future (stochastic uncertainty). One scenario considered by PA is that sometime in the future, someone not knowing about the presence of the WIPP, will inadvertently drill a borehole that intersects the repository. WIPP PA considers several possible release mechanisms that could occur as a direct result of such an event. These include (1) solid waste being released to the surface in the form of drill cuttings and cavings, (2) solid waste particles that spall from the vicinity of the borehole as a result of gas pressure release and are transported to the surface with the circulating drilling fluids, and (3) brine contaminated with dissolved and colloidal radionuclides that flow up the borehole to the surface. This report documents the PA calculations that analyze the probability and consequence of this third release mechanism, which is called Direct Brine Release (DBR). The analysis described in this analysis report was guided by the Analysis Plan AP-137 (Clayton 2008).

3 BACKGROUND

DBRs are releases of contaminated brine originating in the repository and flowing up an intrusion borehole during the period of drilling. In order for DBR to occur, two criteria must be met (Stoelzel and O'Brien 1996):

1. Volume averaged pressure in the vicinity of the repository encountered by drilling must exceed drilling fluid hydrostatic pressure (calculated to be 8 MPa).
2. Brine saturation in the repository must exceed the residual saturation of the waste material (Sampled from a uniform distribution ranging from 0.0 to 0.552).

If both of these criteria are met, DBR is calculated using the multi-phase flow code BRAGFLO with a two dimensional, semi-horizontally oriented grid, which represents the vicinity of the waste panels. If either of these conditions is not satisfied, no DBR is calculated.

DBRs are calculated from the following well deliverability equation in BRAGFLO (Mattax and Dalton 1990):

$$q_p(t) = J_p (P_p(t) - P_{wf}) \quad (1)$$

where $q_p(t)$ is the volumetric brine flux to the well as a function of time, J_p is the well productivity index, $P_p(t)$ is the repository pressure as a function of time, and P_{wf} is the flowing bottom-hole pressure (assumed to be constant during each drilling intrusion). The flowing bottom-hole pressure is defined as the dynamic pressure at the inlet to the wellbore adjacent to the point of entry into the repository. It is less than the static pressure due to elevation, friction and acceleration effects (Stoelzel and O'Brien 1996).

The well productivity index quantifies how readily brine can enter the well and flow to the surface. It is calculated from the following equation (Mattax and Dalton 1990; Chappellear and Williamson 1981):

$$J_p = \frac{2\pi k k_{rp} h}{\mu_p \left[\ln \left(\frac{r_e}{r_w} \right) + s - 0.5 \right]} \quad (2)$$

k = intrinsic permeability of the waste (constant: $2.4 \times 10^{-13} \text{ m}^2$)

k_{rp} = relative permeability of the waste assuming the modified Brooks-Corey relative permeability model: $k_{rp} = S_{el}^{(2+3\lambda)/\lambda}$, where λ is the pore distribution parameter, S_{el} is the effective brine saturation without correction for residual gas saturation $S_{el} = (S_b - S_{br}) / (1 - S_{br})$, S_b is the brine saturation, and S_{br} is the residual brine saturation

h = crushed panel height $h = h_i(1 - \phi) / (1 - \phi)$, where h_i is initial panel height (3.96 m), ϕ is the initial room-scale porosity (0.848), and ϕ is the room-scale porosity at the time of intrusion (calculated by BRAGFLO see Helton et al. (1998))

μ_p = brine viscosity (0.0021 Pa-s)

r_e = external drainage radius of the grid block containing the well ($r_e = \sqrt{(\Delta x)(\Delta y) / \pi}$) where Δx and Δy are the grid cell dimensions of the grid cell containing the well.

r_w = well radius (0.1556 m, assuming a 12.25 in. drill bit diameter)

s = skin factor (enhanced well productivity due to the presence of a cavity at base of well)

The skin factor is calculated (Lee 1982):

$$s = \left(\frac{k}{k_s} - 1 \right) \ln \left(\frac{r_s}{r_w} \right) \quad (3)$$

where k is the permeability of the waste, k_s is the permeability of an open channel as a result of cuttings, cavings and spillings releases (assumed to be infinite) and r_s is the effective radius of the well bore with the cuttings, cavings and spillings volume (V_i) removed.

The effective radius r_s is obtained by converting the cuttings, cavings and spillings volume removed into a cylinder of equal volume with the initial height of the waste (h_i), and then computing the radius of the cylinder:

$$r_s = \sqrt{\frac{V_i}{h_i \pi}} \quad (4)$$

In general, k_s is assumed to be infinite, and Equation (3) can be simplified to:

$$s = (-1) \ln\left(\frac{r_s}{r_w}\right) \quad (5)$$

For the CCA, DBRs were calculated using the code BRAGFLO using a two-dimensional semi-horizontal grid that dips 1° to the south. Five scenarios were simulated, including one “first” intrusion scenario into the undisturbed repository and four “second” or subsequent intrusion scenarios into the previously intruded repository by a borehole. In each scenario, a borehole intrudes the repository and provides a potential conduit for brine flow to the surface. In two of the subsequent intrusion scenarios an additional borehole connects the repository to the Castile brine reservoir. These two scenarios simulate a drilling event (E1 in Salado flow modeling) into the repository that has previously been intruded by a borehole penetrating the Castile, which remains open between the repository and the brine reservoir.

The difference between these two scenarios is the time of the last intrusion (350 and 1,000 years). The other two subsequent intrusion scenarios represent drilling intrusions (E2 in Salado flow modeling) into a repository, which has not experienced a brine reservoir intrusion, with previous intrusion times of 350 and 1,000 years.

For the CCA, two drilling locations were considered: an up-dip location and a down-dip location. The well deliverability equation, Equation (1), was used by the model to calculate a source or sink for brine at the location of the well in the grid. It was assumed that flow within the well was instantaneous. The model was run for a maximum of 11 days and the total volume of brine that reached the well connected to the surface was used to calculate the DBR. The details of the DBR calculations for the CCA are described in Appendix MASS Attachment 16-2 (Stoelzel and O'Brien 1996).

Following the CCA PA calculations, the EPA mandated the Performance Assessment Verification Test (PAVT) (SNL 1997), which consisted of a set of revised parameter values for use in the PA calculations. For the PAVT, BRAGFLO version 4.10 was used for the DBR calculations. In addition, several parameters were changed from the CCA. Specifically, the permeability of the waste was increased from $1.7 \times 10^{-13} \text{ m}^2$ to $2.4 \times 10^{-13} \text{ m}^2$. The permeability of the disturbed rock zone (DRZ) was changed from a constant value of 10^{-15} m^2 to a sampled value (uniform distribution: $10^{-19.4}$ to $10^{-12.5} \text{ m}^2$) and the DRZ was allowed to fracture according to the

fracture model used to represent the consequence of fracturing in the anhydrite marker beds. To implement this sampled permeability for the PAVT the pillars between rooms were assigned the initial sampled permeability while the DRZ surrounding the repository was assigned the permeability at the time of intrusion (possibly enhanced due to fracturing).

Following the PAVT an error in the well productivity index was identified. The 2π term in the numerator, Equation (2), was added (Hadgu et al. 1999). Correcting this error increased the well productivity index and resulted in larger DBR volumes compared to the CCA and PAVT results.

The DBR calculations for the CRA-2004 included several changes from the CCA and PAVT approach. These changes included:

1. Implementation of Option D panel closures in the DBR grid and calculations;
2. Reduction in the extent of the DRZ into the walls of the repository;
3. *Assumption of a constant value for the skin factor instead of having it linked to the spillings release volume;*
4. Adjustments to the way initial conditions (pressure and saturation) are assigned;
5. Addition of a “middle” drilling location;
6. Additional calculation sets as a result of the new drilling location;

and are detailed in Stein et al. (2005).

When the CRA-2004 calculations were being run, the spillings model was being developed, but had not yet completed the necessary peer review process and thus spillings results were not available. This fact necessitated making the Assumption 3 in the list above. Since then, the spillings model has been approved by the peer review panel and updated and qualified results are available for the CRA-2004 PABC calculations. Therefore, for the CRA-2004 PABC results the Assumption 3 in the list above was not implemented. Rather, the actual predicted value of spillings volume released was used to calculate the skin factor as shown in Equations (3)-(5) in the preceding section.

4 APPROACH

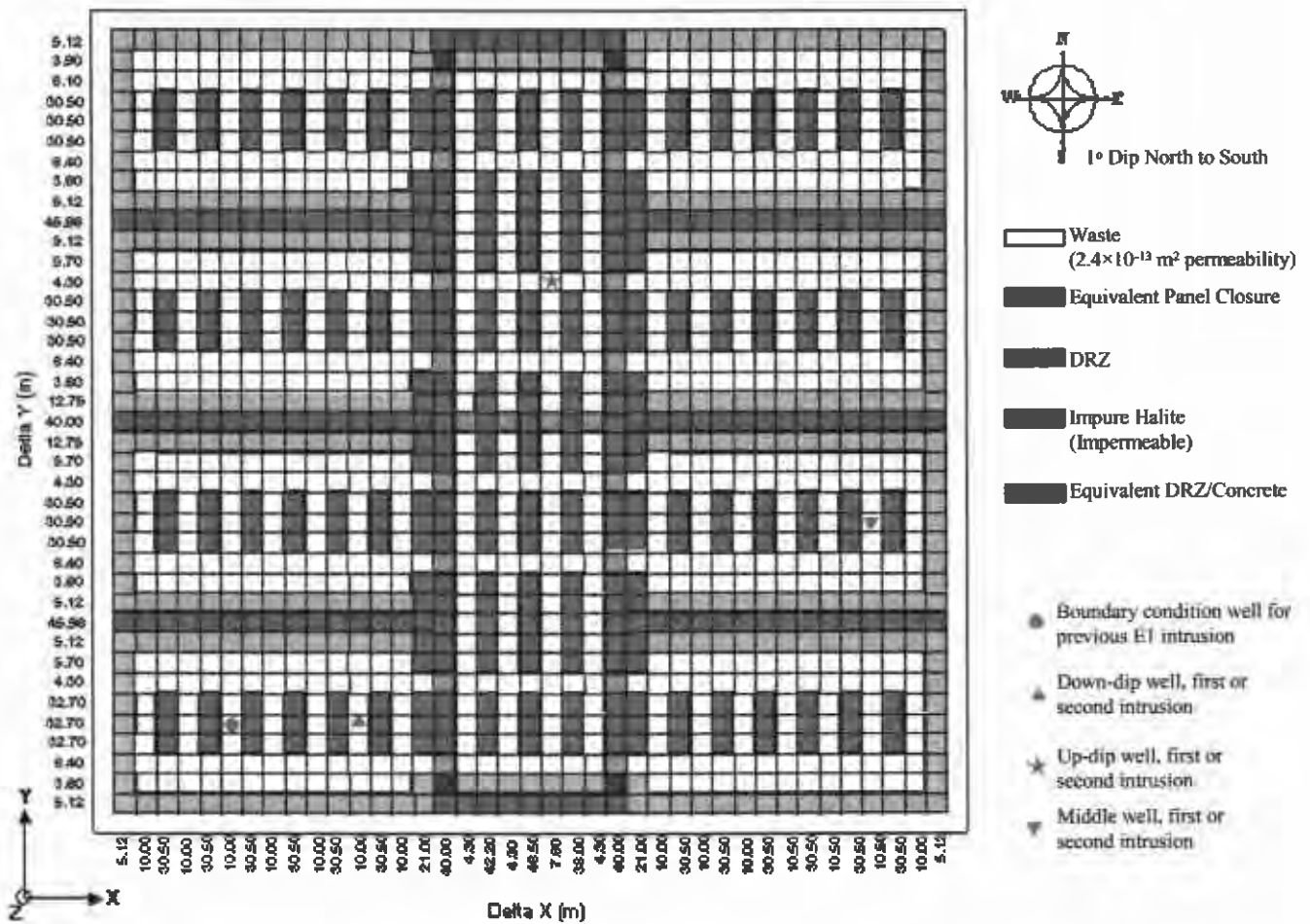
The conceptual models implemented in the DBR calculation for the CRA-2009 PA are unchanged from those used in the CRA-2004 PABC. However, several changes were included in the DBR calculations for the CRA-2009 PA. These are discussed further in Subsection 4.3.

4.1 Model Geometry

The numerical grid, materials and scenarios used for the CRA-2009 PA are the same as were used for the CRA-2004 PABC and is shown in Figure 1. For the CRA-2004 and the CRA-2004 PABC many of the grid cells originally mapped as DRZ in the CCA and PAVT were reassigned to Salado halite. This change ensured that each panel was relatively confined during a DBR intrusion and that little to no gas or brine could flow *around* the panel closures during the runs (Hadgu 2002). This change was presented to and accepted by the Salado Flow Peer Review panel (Caporuscio et al. 2003). The total amount of brine initially available in the pores of the DRZ was conserved between the Salado BRAGFLO runs and the DBR runs for the CRA-2009 PA.

To calculate DBR volumes for the CCA and PAVT two drilling locations were considered: an up-dip and a down-dip location. For the CRA-2004 and CRA-2004 PABC an additional drilling location in the repository was added. The new “middle” drilling location is situated in the eastern panel of Region 2 in the DBR grid (Figure 1). The three drilling locations used in the CRA-2004 PABC are used in the CRA-2009 PA.

Some of the calculations for DBR are for a drilling intrusion that has been preceded by an intrusion in either the same waste panel or a different waste panel. The effects of these prior intrusions are incorporated in the calculations by the specification of a boundary (or initial) condition well as denoted by the red circle in Figure 1. The properties of the boundary condition well depend on the type of intrusion and the time that has passed since the previous intrusion.



Note: Model cells are not to scale. The actual dimensions of the grid blocks are indicated along the edge of the diagram.

Figure 1. CRA-2009 PA DBR material map (logical grid).

4.2 Initial Conditions

Volume averaged pressures and brine saturations are calculated from the 10,000 year BRAGFLO simulations. The BRAGFLO results, corresponding to the time of intrusion, are used in the DBR simulations as initial conditions. For the CCA and PAVT the waste regions in the BRAGFLO grid and the DBR grid were each divided into four regions and volume-averaged pressure and saturations were transferred from corresponding regions in the BRAGFLO grid to the DBR grid. The CRA-2004, CRA-2004 PABC and the CRA-2009 PA DBR calculations used three regions instead of four. These regions corresponded to the single waste panel, south rest of repository (SRR), and north rest of repository (NRR). This method ensured that the relative volumes of these regions were equal between the 10,000 year BRAGFLO runs and the DBR runs.

Figure 2 illustrates the method used to transfer initial conditions in the waste for the CRA-2009 PA DBR runs. The volume averaged pressure and saturation from the three waste-filled regions in the BRAGFLO grid (WAS_AREA, SRR, NRR) at the time of the intrusion are used as the initial pressure and saturation for the three waste regions in the DBR grid (Lower, Middle, and Upper, respectively). The pressure and saturation in the panel closures are also mapped in the same manner. The pressure and saturation then change based on the calculated DBR.

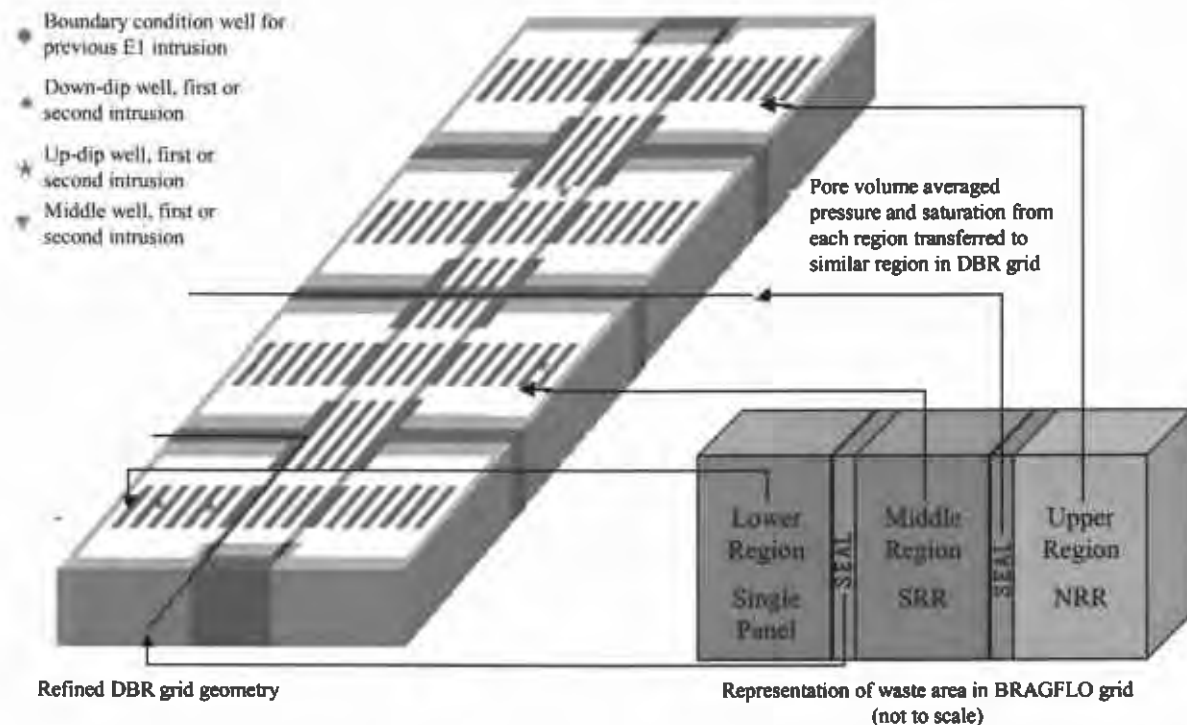


Figure 2. Regions to be used to transfer initial pressure and saturation between the 10,000 year BRAGFLO grid and the DBR grid for the CRA-2009 PA.

4.3 Information Specific to the CRA-2009 PA

As discussed in Analysis Plan AP-137 (Clayton 2008), the CRA-2009 PA contains several updates and corrections to the CRA-2004 PABC. The changes in the DBR calculations are comprised of:

1. Reduction of the maximum DBR duration from 11 to 4.5 days;
2. Updated capillary pressure and relative permeability model;
3. Updated parameter calculations for the well productivity index and material permeabilities;
4. Incorporation of computer code updates;
5. Corrections of the halite and disturbed rock zone porosity values; and
6. Corrections of input file errors.

These changes are discussed in detail below. Item 3 is a deviation from AP-137 (Clayton 2008).

4.3.1 Maximum Direct Brine Release Duration

In the WIPP PA intrusion scenarios, it is hypothesized that brine containing radionuclides could be expelled from repository to the land surface during or directly following the drilling intrusion if repository pressures and brine saturations are sufficiently high (Stoelzel and O' Brien 1996). The duration of a DBR event is constrained by the parameters BLOWOUT:MINFLOW and BLOWOUT:MAXFLOW. The parameter BLOWOUT:MINFLOW represents the minimum DBR duration time, and the parameter BLOWOUT:MAXFLOW represents the maximum DBR duration time. For the CRA-2004 PABC the minimum and maximum DBR durations were set to 3 days and 11 days, respectively.

Analysis Plan for the Modification of the Waste Shear Strength Parameter and Direct Brine Release Parameters, AP-131 (Kirkes and Herrick 2006) describes an analysis that was conducted to reexamine the values of the parameters BLOWOUT:MINFLOW and BLOWOUT:MAXFLOW. The results of the AP-131 analysis showed that the value for BLOWOUT:MAXFLOW should be decreased from 11 days to 4.5 days, while the value for BLOWOUT:MINFLOW should remain at 3 days (Kirkes 2007). The updated maximum DBR duration was used in the CRA-2009 PA.

4.3.2 Capillary Pressure and Relative Permeability Model

In BRAGFLO version 6.0, a cut off saturation is used to determine when the computational cell is effectively dry and no chemical reactions are taking place. The cut off saturation is used to increase code robustness and reduce computational time (Nemer 2007b, 2007d). A modified capillary pressure and relative permeability model (RELP_MOD=12) was developed such that the model would be independent of the cut off saturation value (Nemer 2007b, 2007d). Only the capillary pressure part of the capillary pressure and relative permeability model was modified as the relative permeability model is unchanged from the previous model (RELP_MOD=4). Because of numerical difficulties, capillary pressure has been turned off in the waste-filled areas of the BRAGFLO grid for $t = 0$ to 10,000 years since the

CCA. Thus the use of the modified model would have no impact on the results, but is used for consistency.

Capillary pressure is currently turned off in the WAS_AREA, CONC_PCS and PAN_SL2 materials. The PAN_SL2 material is used as a placeholder, as it has the CONC_PCS material properties with the x- and y-direction properties switched. Thus the choice of capillary-pressure model (i.e. Brooks and Corey 1964, van Genuchten 1978) for these materials has no impact on the results. For future analyses, where capillary-pressure is turned on in the above listed areas, we have assigned the modified capillary pressure and relative permeability model (RELP_MOD=12) to the materials WAS_AREA, CONC_PCS, and PAN_SL2. This particular model was chosen to maintain consistency between the waste panel modeling in the Salado transport calculations and the DBR calculations. Two of the equivalent panel closure materials, CONC_PCS and PAN_SL2 are modeled using a combination of the waste area and concrete properties.

4.3.3 Updated Input Parameter Calculation

Several input parameters for the DBR calculations are derived in the second ALGEBRACDB calculation step. Modifications to the calculation procedure were made for the CRA-2009 PA DBR calculations to maintain consistency in the well productivity index and permeability parameters. Details of the changes can be found in the ALGEBRACDB input files, ALG2_DBR_CRA09_Ss.INP (where $s = 1..5$) which are located in CMS in library LIBCRA09_DBR.

The well productivity index, as shown in Equation (2), is calculated from r_e , the external drainage radius of the grid block containing the well where Δx and Δy are the grid cell dimensions of the grid cell containing the well. The $\ln(r_e/r_w)$ term is used to account for the difference between the grid cell size and the borehole size. If the grid cell is the same size as the borehole, then the $\ln(r_e/r_w)$ term becomes zero. As the grid cell increases, this term is larger, which will reduce the well productivity index calculated by Equation (2).

For the CRA-2004 PABC, it was assumed that $r_e = \sqrt{(10)(32.7)/\pi} = 10.2$ m, which corresponds to the dimensions of the grid block corresponding to the down-dip well (Figure 1). The same r_e was used for all three drilling locations. Using $r_e = 10.2$ m and $r_w = 0.1556$ m gives $\ln(r_e/r_w) = 4.18$. For the CRA-2009 PA, r_e was calculated for each drilling location using the corresponding grid cell dimensions. The grid cells for the middle and upper drilling locations are smaller than the lower drilling location grid cell, which will result in a lower r_e . As seen in Equation (2), a lower r_e will result in higher volumes. The CRA-2009 PA used a r_e of 10.2 m ($\sqrt{(10)(32.7)/\pi}$), 10.1 m ($\sqrt{(10.5)(30.5)/\pi}$) and 3.2 m ($\sqrt{(7.6)(4.3)/\pi}$) for the lower, middle and upper drilling locations, respectively.

As the value of r_e for the lower drilling location remains the same, there is no effect on the lower drilling intrusion DBR calculations. Using the updated value of r_e for the middle drilling location gives $\ln(r_e/r_w) = 4.17$, which is a ~0.2% change. Therefore, there is a minimal effect on the middle drilling intrusion DBR calculations using the updated value of r_e .

The updated value of r_e for the upper drilling location changed the most and results in $\ln(r_e/r_w) = 3.03$. Using the average cuttings and cavings area of 0.25 m^2 (Ismail 2008) gives $r_s = 0.22$ and a skin factor of -0.60 . Comparing the denominator in Equation (2) for the previous and updated value of r_e for the upper drilling location and using the average skin factors gives that the well productivity index for the upper drilling location could increase by $\sim 60\%$. An increase in the well productivity index will increase the brine flow, which will then decrease the pressure in the intruded panel and reduce the brine flow, so the effect of the update is not easily determined.

The S_HALITE material permeability is a sampled parameter and is determined by the permeability value used in the corresponding BRAGFLO calculation. For the CRA-2004 PABC DBR calculations, the x-permeability was set to the corresponding value in the BRAGFLO calculations, but the y- and z-permeability were not changed from the mean value of the distribution. For the CRA-2009 PA, the S_HALITE material x-, y- and z-permeabilities are updated to reflect the values used in the corresponding BRAGFLO calculations. As the S_HALITE material permeability is low (10^{-21} to 10^{-24} m^2), there is effectively no brine or gas transport within the 4.5 days. Therefore, the update to the S_HALITE material permeability calculations does not affect the DBR calculations, but is needed for consistency.

For the panel closure materials, CONC_PCS, DRZ_CONC and PAN_SL2, equivalent permeabilities are used. The PAN_SL2 material is used as a placeholder, as it has the CONC_PCS material properties with the x- and y-direction properties switched. As the panel closure materials are represented by one grid cell in the DBR grid (Figure 1), the permeability is calculated as the equivalent permeability of the various panel closure materials in series or in parallel depending on the orientation of the panel closures in the grid. In the equivalent permeability calculations for the CRA-2004 PABC, multiplying two low permeabilities could generate an equivalent permeability of zero for some cases due to round off error. The equation that can result in an equivalent permeability (κ_{eq}) of zero for some cases is:

$$\kappa_{eq} = \frac{(L_1 + L_2)\kappa_1\kappa_2}{L_2\kappa_1 + L_1\kappa_2} \quad (6)$$

where κ_1 and κ_2 are the permeabilities of materials 1 and 2 and L_1 and L_2 thicknesses of materials 1 and 2. An equivalent permeability of zero was found to arise when the numerator was below $\sim 3 \times 10^{-39}$. As low permeabilities are needed for this to occur, there is effectively no transport within the 4.5 days. Therefore, the update to the equivalent permeability calculation will not affect the DBR calculations, but is needed for consistency.

For the CRA-2009 PA, the equivalent permeability calculations were updated to avoid the calculation of an equivalent permeability of zero. This was accomplished by multiplying the permeabilities used in the equivalent permeability calculations by a constant factor (10^{10}) and then dividing the final results by the same factor. The results of the modified equations were compared with hand calculations to confirm the proper implementation.

4.3.4 *Computer Code Updates*

DBR volumes are calculated using the BRAGFLO suite of codes (PREBRAG, BRAGFLO, POSTBRAG), in conjunction with several utility codes (Long 2008). The DBR calculations for the CRA-2004 PABC used PREBRAG version 7.0, BRAGFLO version 5.0 and POSTBRAG version 4.00. BRAGFLO version 6.0 was developed to incorporate additional capabilities and improve code robustness (Nemer 2007b, 2007d). As BRAGFLO version 6.0 includes more input parameters and capabilities, an updated version of PREBRAG (8.0) was developed (Gilkey 2007). Furthermore, while developing test cases for BRAGFLO version 6.0, an error was encountered in POSTBRAG version 4.00 (Nemer 2007c). A dynamic array was sized incorrectly which caused some data or data labels to be written incorrectly. POSTBRAG version 4.00A (Nemer 2007a) was developed to remedy this problem.

For the DBR calculations in the CRA-2009 PA, the codes PREBRAG version 8.0, BRAGFLO version 6.0 and POSTBRAG version 4.00A were used. The modifications to the BRAGFLO code were turned off for the DBR calculations, as they are not needed. The PREBRAG input files were modified to be consistent with PREBRAG version 8.0, with all other options the same as were used in the CRA-2004 PABC.

4.3.5 *Halite/Disturbed Rock Zone Porosity*

An error in the determination of the intact halite porosity variable, S_HALITE:POROSITY, was discovered and reported in Parameter Problem Report 2007-002 (Ismail 2007a). The maximum of the range was taken from data reported in weight fraction without the conversion to volume fraction. Converting the maximum value from a weight fraction to a volume fraction changed the value from 0.030 to 0.0519 (Ismail 2007b). The minimum and mode values of the distribution were not affected. Furthermore, current WIPP PA practice for determining the disturbed rock zone (DRZ) porosity is to increase the S_HALITE:POROSITY value by 0.0029. Therefore, the maximum value of the range for the DRZ_0:POROSITY, DRZ_1:POROSITY and DRZ_PCS:POROSITY parameters increased from 0.0329 to 0.0548. The CRA-2009 PA used the corrected porosity ranges.

4.3.6 *Input File Corrections*

Two inconsistencies were discovered in the input files used by the ALGEBRACDB code as part of the DBR calculations (Clayton 2007). The first inconsistency involved the input file used to set up the boundary conditions for the S3 scenario calculations. The S3 scenario consists of an intrusion through the repository and a brine pocket, 1,000 years after closure. The intrusion time in the input file was incorrectly assigned the value of 350 years instead of 1,000 years. The second inconsistency entailed the limits of integration used to calculate the DBR volume. The integration limit was determined by a logic command of “if less than zero” when it should have used “if less than or equal to zero”. For more details on the input file changes, as well as the impact of the changes, see Clayton (2007). The CRA-2009 PA will include the corrections to the DBR calculation input files.

5 CALCULATION METHODOLOGY

DBR calculations are divided into five scenarios. Each DBR scenario represents an intrusion into the repository due to a drilling event. The initial conditions for the DBR simulations are obtained from the BRAGFLO Salado Flow simulations (Nemer and Clayton 2008) using an appropriate scenario (depending on the intrusion type E1 or E2) and at an appropriate time for the particular drilling intrusion time. An E1 intrusion scenario is defined as an intrusion into the repository, which creates a pathway to a pressurized brine pocket below the repository. An E2 intrusion scenario is defined as an intrusion into the repository that does not create a pathway to a pressurized brine pocket below the repository. The results of the DBR calculations are the volumes of brine that leave the repository and reach the surface at the time of drilling and up to 4.5 days after. These results are used by the code CCDFGF (Hansen 2003) to interpolate volumes of waste for the specific conditions that arise in a given future (location and timing of future drilling intrusions). See the Design Document for CCDFGF (Hansen 2003) for details on how the DBR scenarios are used to calculate releases.

5.1 Modeled Scenarios

Below an overview is given of the DBR calculations performed for the CRA-2009 PA. In performing DBR calculations, the five BRAGFLO scenarios S1-S5 are used as initial conditions for the DBR calculations. These initial conditions along with DBR simulations cover a range of possible numbers of intrusions, locations and timing. A summary of intrusion times for each scenario is given in Table 5-1.

Table 5-1. Intrusion times modeled by DBR for each scenario.

Scenario	Intrusion times (years)
S1	100, 350, 1000, 3000, 5000, 10000
S2	550, 750, 2000, 4000, 10000
S3	1200, 1400, 3000, 5000, 10000
S4	550, 750, 2000, 4000, 10000
S5	1200, 1400, 3000, 5000, 10000

5.1.1 Scenario 1 (S1)

The BRAGFLO Salado modeling results from the S1 scenario are used as initial conditions to construct the first intrusion into the repository in which a DBR may occur. In BRAGFLO Salado modeling (Nemer and Clayton 2008), this scenario represents an undisturbed repository. Upper, middle, and lower drilling intrusions are modeled at 100, 350, 1,000, 3,000, 5,000, and 10,000 years (3 locations \times 6 intrusion times \times 100 vectors = 1,800 calculations per replicate).

5.1.2 Scenario 2 (S2)

The BRAGFLO Salado modeling results from the S2 scenario are used as initial conditions to construct a second or subsequent intrusion into the repository in which a DBR may occur and in which the first intrusion had hit a Castile brine reservoir at 350 years (Nemer and Clayton 2008). For the second or subsequent intrusion, upper, middle, and lower drilling intrusions were modeled at 550, 750, 2,000, 4,000 and 10,000 years (3 locations \times 5 intrusion times \times 100 vectors = 1,500 calculations per replicate). The effect of the prior E1 intrusion is incorporated in the calculations by the specification of a boundary condition well as denoted by the red circle in Figure 1. The properties of the boundary condition well correspond to the properties at the time of the second intrusion.

Runs for the lower drilling location assume that the second or subsequent intrusion occurs at the location labeled in Figure 1 as the “down-dip well”. This represents an intrusion in the same panel that was intersected by a previous intrusion (assumed to be at the location labeled “boundary condition well”) and therefore the abandoned borehole still connects the panel with the brine reservoir. Runs for the middle drilling location assume that the second or subsequent intrusion occurs at the location labeled in Figure 1 as the “middle well”; a previous intrusion is assumed to have occurred at the location labeled “boundary condition well,” which is in an adjacent panel. Runs for the upper drilling location assume that the second or subsequent intrusion occurs at the location labeled “up-dip well” in Figure 1; a previous intrusion is assumed to have occurred at the location labeled “boundary condition well,” which is in a panel that is not adjacent to the current intrusion.

5.1.3 Scenario 3 (S3)

The BRAGFLO Salado modeling results from the S3 scenario are used as initial conditions to construct a second or subsequent intrusion into the repository in which a DBR may occur and in which the first intrusion had hit a Castile brine reservoir at 1,000 years (Nemer and Clayton 2008). Upper, middle, and lower second or subsequent intrusions are modeled at 1,200, 1,400, 3,000, 5,000 and 10,000 years (3 locations \times 5 intrusion times \times 100 vectors = 1,500 calculations per replicate). The effect of the prior E1 intrusion and the lower, middle, and upper drilling locations are treated the same as for the S2 scenario.

5.1.4 Scenario 4 (S4)

The BRAGFLO Salado modeling results from the S4 scenario are used as initial conditions to construct a second or subsequent intrusion into the repository in which a DBR may occur and in which the first intrusion occurs at 350 years without hitting a Castile brine reservoir (Nemer and Clayton 2008). Upper, middle, and lower second or subsequent intrusions are modeled at 550, 750, 2,000, 4,000 and 10,000 years (3 locations \times 5 intrusion times \times 100 vectors = 1,500 calculations per replicate). Runs for the lower drilling location assume the second or subsequent intrusion occurs at the location labeled in Figure 1 as the “down-dip well”. This represents an intrusion into the same panel that was intersected by a previous E2 intrusion. The borehole from the previous intrusion is not represented explicitly in the model. Runs for the

middle drilling location assume that the second or subsequent intrusion occurs at the location labeled in Figure 1 as the “middle well.” Runs for the upper drilling location assume that the second or subsequent intrusion occurs at the location labeled “up-dip well” in Figure 1.

5.1.5 Scenario 5 (S5)

The BRAGFLO Salado modeling results from the S5 scenario are used as initial conditions to construct a second or subsequent intrusion into the repository in which a DBR may occur and in which the first intrusion occurs at 1,000 years without hitting a Castile brine reservoir (Nemer and Clayton 2008). Upper, middle, and lower second or subsequent intrusions are modeled at 1,200, 1,400, 3,000, 5,000 and 10,000 years (3 locations × 5 intrusion times × 100 vectors = 1,500 calculations per replicate). The lower, middle, and upper drilling locations are treated the same as for the S4 scenario.

5.2 Computational Modeling Process

The run control procedures followed for the CRA-2009 PA are documented in Long (2008). There are four groups of codes that have to be run to complete DBR calculations. These groups are described below. Locations of the input files for the CRA-2009 PA are listed below in terms of a VMS CMS library and class.

5.2.1 Grid Generation and Material Assignments

This group was run once for the CRA-2009 PA.

5.2.1.1 GENMESH

GENMESH defines the numerical grid used in the DBR calculations. This grid is shown in Figure 1. It is the same as was used in the CCA and PAVT. For the CRA-2009 PA, the input file for this step is GM_DBR_CRA09.INP and is stored in CMS library LIBCRA09_DBR, class CRA09-0.

5.2.1.2 MATSET

MATSET assigns material properties from the parameter database, which are needed by codes listed in the steps below. Properties that vary for each vector are assigned median values by MATSET and then are overwritten in later steps. For the CRA-2009 PA, the input file for this step is MS_DBR_CRA09.INP and is stored in CMS library LIBCRA09_DBR, class CRA09-0.

5.2.2 Initial Conditions, Sampled and Calculated Input Parameters

This part of the calculation was run once for each vector-time-scenario combination (600 times for the S1 scenario and 500 times each for the S2-S5 scenarios).

5.2.2.1 ALGEGRACDB STEP 1 (ALG1)

In this step, ALGEGRACDB reads CAMDAT output files produced by CUTTINGS_S and outputs CAMDAT files with information about the pressure, saturation, porosity, and crushed panel height, which is used as initial conditions for DBR calculations. Furthermore, the spillings volume for each vector-scenario-time combination is transferred in this step. This is how volume averaged BRAGFLO results are transferred to the DBR calculations. For the CRA-2009 PA, the input file for this step is ALG1_DBR_CRA09.INP and is stored in CMS library LIBCRA09_DBR, class CRA09-0.

5.2.2.2 RELATE STEP 1 (RELATE1)

In this step, RELATE transfers material properties and results from one grid to another. In the first RELATE step, volume-averaged porosity, pressure, and saturation are transferred from the ALGEGRACDB step 1 files which originated from the CUTTINGS_S output files, as described in section 5.2.2.1, to the DBR grid. For the CRA-2009 PA, the input file for this step is REL1_DBR_CRA09.INP and is stored in CMS library LIBCRA09_DBR, class CRA09-0.

5.2.2.3 RELATE STEP 2 (RELATE2)

In the second RELATE step the material properties are transferred from the BRAGFLO grid to the DBR grid. The material properties that are transferred in this step include material properties that may change during a 10,000 year BRAGFLO run (i.e. permeability of the DRZ due to fracturing). The material properties transferred are the material properties at the various intrusion times. Also, material properties that are modified in the preprocessing steps of BRAGFLO are transferred in this step. For the CRA-2009 PA, the input files for this step are REL2_DBR_CRA09_Ss.INP where $s = 1...5$, and are stored in CMS library LIBCRA09_DBR, class CRA09-0.

5.2.2.4 ICSET

In this step, ICSET assigns the initial pressure and saturations gathered from ALGEGRACDB step 1, RELATE step 1, and RELATE step 2. For the CRA-2009 PA, the input files for this step are IC_DBR_CRA09_Ss.INP where $s = 1..5$, and are stored in CMS library LIBCRA09_DBR, class CRA09-0.

5.2.2.5 ALGEGRACDB STEP 2 (ALG2)

In this step, ALGEGRACDB is used to calculate parameters that are required by the BRAGFLO code used to run DBR. This step involves many calculations that are defined in the input file. A partial list of calculations performed in this step includes:

1. Material properties are converted to units needed by BRAGFLO;
2. Equivalent permeabilities of the panel closure materials are calculated;
3. Flowing bottomhole pressure and well productivity index are calculated;
4. Grid cell elevations are calculated to account for the one-degree dip;

5. If both criteria (pressure > 8 MPa; mobile saturation > 1) are met, then the maximum number of time steps is set to equal 1000, allowing BRAGFLO to calculate the magnitude of the DBR volume. If either criterion is not met, the maximum number of time steps is set equal to 1, which effectively means that BRAGFLO will calculate no volume for that instance.

For the CRA-2009 PA, the input files for this step are ALG2_DBR_CRA09_Ss.INP where $s = 1...5$, and are stored in CMS library LIBCRA09_DBR, class CRA09-0.

5.2.3 Calculation of Direct Brine Release Volumes

This part of the calculation was run once for each vector-time-drilling location-scenario combination (1,800 times for the S1 scenario and 1,500 times each for the S2-S5 scenarios).

5.2.3.1 PREBRAG

In this step, PREBRAG produces BRAGFLO input files from the output files from ALGEBRACDB step 2. For the CRA-2009 PA, the input files for this step are BF1_DBR_CRA09_Ss_c.INP where $s = 1...5$, $c = L, M, U$, and are stored in CMS library LIBCRA09_DBR, class CRA09-0.

5.2.3.2 BRAGFLO

In this step, BRAGFLO calculates the flow of gas and brine in the DBR grid for the duration of the drilling event (no more than 4.5 days). For the CRA-2009 PA, the input files for this step are BF2_DBR_CRA09_Rr_Ss_Ttttt_c_Vvvv.INP where $r = 1...3$, $s = 1...5$, $ttttt =$ intrusion time listed in Table 5-1 for each scenario, $c = L, M, U$, $vvv = 001... 100$, and are stored in CMS library LIBCRA09_DBRrSs, class CRA09-0.

5.2.3.3 POSTBRAG

In this step, POSTBRAG converts the output of BRAGFLO to a CAMDAT file. This step has no input file.

5.2.4 Post-Processing of Results

The binary CAMDAT files produced by POSTBRAG need to be post-processed to extract the cumulative DBR volume at the surface for each simulated intrusion. This post-processing is done in two steps described below.

5.2.4.1 ALGEBRACDB STEP 3 (ALG3)

In this step, ALGEBRACDB is used to calculate the cumulative brine flow up the borehole over the drilling period. This cumulative brine volume is the direct brine released to the surface and is used by the code CCDFGF to calculate the DBR CCDF. ALGEBRACDB was run once for each vector-time-drilling location-scenario combination (1,800 times for the S1 scenario

and 1,500 times each for the S2-S5 scenarios) for a total of 7,800 runs. For the CRA-2009 PA, the input file for this step is ALG3_DBR_CRA09.INP and is stored in CMS library LIBCRA09_DBR, class CRA09-0.

5.2.4.2 SUMMARIZE

SUMMARIZE tabulates the results stored in CAMDAT files and outputs ASCII tables which are needed by CCDFGF. This step is run 78 times per replicate (once per time-drilling location-scenario combination). Each of the resulting tables lists cumulative brine volumes for 100 vectors which is then used in further calculations. For the CRA-2009 PA, the input files for this step are SUM_DBR_CRA09_Rr_Ss_Ttttt_c.INP and is stored in CMS library LIBCRA09_SUM class CRA09-0, where $r = 1...3$, and $s = 1...5$, tttt is one of the intrusion times listed in Table 5-1 for each scenario, and $c = L,M,U$.

6 RESULTS

The DBR calculations for replicate 1 of the CRA-2009 PA are presented in this section and compared with results from replicate 1 of the CRA-2004 PABC. The analysis of the CRA-2004 PABC results is described in an earlier report (Stein et al. 2005) and will only be summarized here as appropriate.

Each set of DBR calculations resulted in 7,800 (1,800 for first intrusion and $1,500 \times 4 = 6,000$ for second intrusion) separate vector-scenario-drilling location-time combinations. These results are input into the code CCDFGF, which then calculates a release for any vector-intrusion time combination. This is done by first, linearly interpolating modeled volumes between the fixed intrusion times (Table 5-1) and second, multiplying the resulting intrusion-specific DBR volume with the radionuclide concentration calculated for that vector and intrusion time by the code PANEL (Garner and Leigh, 2005).

The present analysis report only covers results from replicate 1. The replicate variability is not expected to be significant as the average initial conditions (pressure, saturation) used in the DBR calculations are only slightly different between the three replicates. This is shown in section 6.5 of the CRA-2009 PA BRAGFLO analysis report (Nemer and Clayton 2008). For consistency with previous analyses, non-zero volumes are defined as volumes that are greater than 10^{-7} m^3 .

6.1 Summary

In this section, results from the CRA-2009 PA and the CRA-2004 PABC are compared. Table 6-1 compares some summary statistics for the calculations. While the CRA-2009 PA resulted in an increase in the number of non-zero DBR volumes over the CRA-2004 PABC, the overall maximum DBR volume decreased from 68.9 m^3 to 58.8 m^3 . For the CRA-2009 PA, two vectors (Vector 3 and 74) have DBR volumes equal to zero calculated in all of the scenarios and therefore DBR will not contribute to the total releases calculated for those vectors. The same two vectors were observed with the same behavior in the CRA-2004 PABC. The maximum volume of 58.8 m^3 occurred for Vector 6, S2 scenario, lower drilling intrusion, time = 10,000 yrs.

Table 6-1. Summary of differences between DBR calculations.

	CRA-2009 PA	CRA-2004 PABC
Total number of model runs	7,800	7,800
Number non-zero DBR volumes	1,001	721
Maximum DBR volume for scenario S1 (m ³)	1.94E+01	1.80E+01
Maximum DBR volume for scenario S2 (m ³)	5.88E+01	6.89E+01
Maximum DBR volume for scenario S3 (m ³)	4.35E+01	6.40E+01
Maximum DBR volume for scenario S4 (m ³)	1.86E+01	1.41E+01
Maximum DBR volume for scenario S5 (m ³)	2.12E+01	1.41E+01

Note: The volume of direct brine released was obtained from the output variable BRIN_REL which is calculated in the ALGEBRACDB step 3 post processing step, see section 5.2.4.1, and contained in the ALG3 CDB files.

6.2 Direct Brine Releases from the Lower Drilling Location

Table 6-2 through Table 6-6 summarizes the number of vectors in the CRA-2009 PA that had a non-zero DBR volume and the maximum and average DBR volumes for each scenario-time-drilling location combination. The same data for the CRA-2004 PABC is shown for comparison.

One important result that is evident from Table 6-2 through Table 6-6 is that are DBRs less likely to occur during middle and upper drilling intrusions when compared with the lower drilling location. Of all non-zero DBR volumes for the CRA-2009 PA, approximately 67% occurred during a lower drilling intrusion, 18% during a middle drilling intrusion, and 16% during an upper drilling intrusion. Furthermore, of the non-zero DBR volumes that occur during a lower drilling intrusion, 83% are found in scenarios S2 and S3. Therefore, the majority of the non-zero DBR volumes occur when there is a previous E1 intrusion within the same panel.

Not only are DBRs less likely to occur during middle and upper drilling intrusions, but also the DBR volumes from such intrusions tend to be much smaller than DBR volumes from lower drilling intrusions. For the CRA-2009 PA, the maximum DBR volume for the middle drilling location is 20.6 m³ (Vector 82, S2 scenario, at time = 4,000 years) and only 12.5 m³ for the upper drilling location (Vector 69, S5 scenario, at time = 1,400 years). For these reasons, this report only examines in detail the lower drilling intrusions.

Table 6-2. Summary table of number of vectors with non-zero, maximum and average DBR volumes for the S1 DBR calculations.

Scenario	Time [yrs]	Drilling Location	Number of Vectors		Max volume (m ³)		Average volume (m ³)	
			CRA-2009 PA	CRA-2004 PABC	CRA-2009 PA	CRA-2004 PABC	CRA-2009 PA	CRA-2004 PABC
S1	100	L	0	0	0.00E+00	0.00E+00	0.00E+00	0.00E+00
S1	350	L	0	0	0.00E+00	0.00E+00	0.00E+00	0.00E+00
S1	1,000	L	11	5	1.24E+01	1.51E+00	1.86E-01	1.52E-02
S1	3,000	L	14	6	5.53E+00	1.09E+00	1.30E-01	2.14E-02
S1	5,000	L	14	10	1.56E+01	1.96E+00	3.14E-01	3.75E-02
S1	10,000	L	15	11	1.94E+01	1.80E+01	3.33E-01	2.11E-01
S1	100	M	0	0	0.00E+00	0.00E+00	0.00E+00	0.00E+00
S1	350	M	0	0	0.00E+00	0.00E+00	0.00E+00	0.00E+00
S1	1,000	M	9	2	1.83E+00	2.70E-04	3.74E-02	2.76E-06
S1	3,000	M	9	5	1.86E+00	2.82E-01	4.47E-02	2.98E-03
S1	5,000	M	8	4	9.58E+00	4.20E-01	1.14E-01	5.52E-03
S1	10,000	M	8	3	1.37E+00	1.02E-01	2.78E-02	1.05E-03
S1	100	U	0	0	0.00E+00	0.00E+00	0.00E+00	0.00E+00
S1	350	U	0	0	0.00E+00	0.00E+00	0.00E+00	0.00E+00
S1	1,000	U	9	1	1.37E+00	8.88E-06	2.80E-02	8.88E-08
S1	3,000	U	9	4	1.30E+00	1.68E-01	3.27E-02	1.79E-03
S1	5,000	U	7	3	9.77E-01	7.76E-02	1.13E-02	7.80E-04
S1	10,000	U	9	3	8.59E-01	6.35E-02	1.68E-02	6.54E-04

Note: Volume releases less than $1 \times 10^{-7} \text{ m}^3$ have been reduced to 0.0 for the purposes of this table and the average DBR volume is calculated by the total of the DBR volumes divided by the total number of vectors. The DBR volume was obtained from the output variable BRIN_REL which is calculated in the ALGEBRACDB step 3 post processing step, see section 5.2.4.1, and contained in the ALG3 CDB files.

Table 6-3. Summary table of number of vectors with non-zero, maximum and average DBR volumes for the S2 DBR calculations.

Scenario	Time [yrs]	Drilling Location	Number of Vectors		Max volume (m ³)		Average volume (m ³)	
			CRA-2009 PA	CRA-2004 PABC	CRA-2009 PA	CRA-2004 PABC	CRA-2009 PA	CRA-2004 PABC
S2	550	L	96	96	3.46E+01	4.37E+01	1.20E+01	1.23E+01
S2	750	L	84	85	3.21E+01	4.83E+01	1.14E+01	1.14E+01
S2	2,000	L	53	54	3.24E+01	5.54E+01	7.53E+00	8.75E+00
S2	4,000	L	42	46	4.07E+01	6.50E+01	5.63E+00	5.75E+00
S2	10,000	L	47	47	5.88E+01	6.89E+01	6.58E+00	6.77E+00
S2	550	M	4	2	4.19E+00	1.87E-02	4.84E-02	1.87E-04
S2	750	M	7	1	2.15E+00	3.05E-04	3.05E-02	3.05E-06
S2	2,000	M	8	4	6.59E+00	1.61E+00	1.76E-01	1.73E-02
S2	4,000	M	9	5	2.06E+01	2.32E-01	2.43E-01	2.83E-03
S2	10,000	M	7	4	1.76E+00	1.26E-01	4.01E-02	1.44E-03
S2	550	U	3	1	3.28E-01	5.80E-06	4.62E-03	5.79E-08
S2	750	U	4	1	1.94E+00	1.22E-03	2.04E-02	1.22E-05
S2	2,000	U	8	3	5.71E+00	6.67E-01	1.30E-01	7.74E-03
S2	4,000	U	7	5	9.74E-01	8.38E-02	1.62E-02	8.50E-04
S2	10,000	U	6	3	8.80E-01	6.62E-02	1.83E-02	6.87E-04

Note: Volume releases less than $1 \times 10^{-7} \text{ m}^3$ have been reduced to 0.0 for the purposes of this table and the average DBR volume is calculated by the total of the DBR volumes divided by the total number of vectors. The DBR volume was obtained from the output variable BRIN_REL which is calculated in the ALGEBRACDB step 3 post processing step, see section 5.2.4.1, and contained in the ALG3 CDB files.

Table 6-4. Summary table of number of vectors with non-zero, maximum and average DBR volumes for the S3 DBR calculations.

Scenario	Time [yrs]	Drilling Location	Number of Vectors		Max volume (m ³)		Average volume (m ³)	
			CRA-2009 PA	CRA-2004 PABC	CRA-2009 PA	CRA-2004 PABC	CRA-2009 PA	CRA-2004 PABC
S3	1,200	L	77	74	2.95E+01	6.40E+01	8.01E+00	9.03E+00
S3	1,400	L	53	54	2.37E+01	3.90E+01	4.97E+00	5.39E+00
S3	3,000	L	35	28	2.76E+01	3.85E+01	2.67E+00	3.25E+00
S3	5,000	L	32	27	4.04E+01	4.69E+01	3.09E+00	3.92E+00
S3	10,000	L	31	25	4.35E+01	2.83E+01	2.48E+00	2.39E+00
S3	1,200	M	11	3	1.70E+01	7.12E-01	3.12E-01	7.14E-03
S3	1,400	M	12	3	1.30E+01	4.59E-01	2.51E-01	4.59E-03
S3	3,000	M	9	4	3.49E+00	2.82E-01	7.37E-02	2.98E-03
S3	5,000	M	10	3	1.03E+01	1.26E-01	1.31E-01	1.28E-03
S3	10,000	M	7	3	1.43E+00	1.06E-01	3.21E-02	1.12E-03
S3	1,200	U	9	1	4.53E-01	1.14E-03	8.15E-03	1.14E-05
S3	1,400	U	10	2	1.25E+01	2.12E-04	2.04E-01	2.14E-06
S3	3,000	U	8	5	1.63E+00	1.51E-01	3.96E-02	1.66E-03
S3	5,000	U	8	2	9.45E-01	7.36E-02	1.30E-02	7.42E-04
S3	10,000	U	5	3	8.73E-01	6.52E-02	1.76E-02	6.78E-04

Note: Volume releases less than $1 \times 10^{-7} \text{ m}^3$ have been reduced to 0.0 for the purposes of this table and the average DBR volume is calculated by the total of the DBR volumes divided by the total number of vectors. The DBR volume was obtained from the output variable BRIN_REL which is calculated in the ALGEBRACDB step 3 post processing step, see section 5.2.4.1, and contained in the ALG3 CDB files.

Table 6-5. Summary table of number of vectors with non-zero, maximum and average DBR volumes for the S4 DBR calculations.

Scenario	Time [yrs]	Drilling Location	Number of Vectors		Max volume (m ³)		Average volume (m ³)	
			CRA-2009 PA	CRA-2004 PABC	CRA-2009 PA	CRA-2004 PABC	CRA-2009 PA	CRA-2004 PABC
S4	550	L	3	2	9.05E-01	7.14E-04	1.09E-02	7.16E-06
S4	750	L	2	1	1.86E+01	2.68E+00	1.86E-01	2.68E-02
S4	2,000	L	5	3	7.17E+00	2.40E+00	7.30E-02	2.40E-02
S4	4,000	L	7	3	3.03E+00	3.57E-01	5.03E-02	3.69E-03
S4	10,000	L	7	5	1.46E+01	1.41E+01	2.32E-01	1.57E-01
S4	550	M	4	1	4.42E+00	1.00E-05	5.08E-02	1.00E-07
S4	750	M	5	1	2.47E+00	1.93E-03	2.78E-02	1.93E-05
S4	2,000	M	4	0	5.11E+00	0.00E+00	6.00E-02	0.00E+00
S4	4,000	M	6	2	1.62E+00	1.58E-01	3.46E-02	1.59E-03
S4	10,000	M	5	1	1.42E+00	1.01E-01	2.28E-02	1.01E-03
S4	550	U	3	1	3.27E-01	5.84E-06	4.56E-03	5.84E-08
S4	750	U	4	1	1.68E+00	1.22E-03	1.77E-02	1.22E-05
S4	2,000	U	5	1	6.21E+00	6.53E-02	1.05E-01	6.53E-04
S4	4,000	U	5	4	1.04E+00	9.60E-02	1.69E-02	9.76E-04
S4	10,000	U	5	1	9.02E-01	6.23E-02	1.41E-02	6.23E-04

Note: Volume releases less than 1×10^{-7} m³ have been reduced to 0.0 for the purposes of this table and the average DBR volume is calculated by the total of the DBR volumes divided by the total number of vectors. The DBR volume was obtained from the output variable BRIN_REL which is calculated in the ALGEBRACDB step 3 post processing step, see section 5.2.4.1, and contained in the ALG3 CDB files.

Table 6-6. Summary table of number of vectors with non-zero, maximum and average DBR volumes for the S5 DBR calculations.

Scenario	Time [yrs]	Drilling Location	Number of Vectors		Max volume (m ³)		Average volume (m ³)	
			CRA-2009 PA	CRA-2004 PABC	CRA-2009 PA	CRA-2004 PABC	CRA-2009 PA	CRA-2004 PABC
S5	1,200	L	13	7	2.12E+01	2.06E+00	3.74E-01	2.58E-02
S5	1,400	L	5	3	1.23E+01	1.12E-01	1.61E-01	1.23E-03
S5	3,000	L	7	3	2.96E+00	6.45E-01	4.40E-02	6.45E-03
S5	5,000	L	6	4	4.41E+00	1.24E+00	7.32E-02	1.54E-02
S5	10,000	L	7	5	1.45E+01	1.41E+01	2.36E-01	1.57E-01
S5	1,200	M	10	3	1.71E+01	7.02E-01	1.83E-01	7.02E-03
S5	1,400	M	9	3	1.29E+01	4.63E-01	2.40E-01	4.65E-03
S5	3,000	M	7	2	3.80E+00	2.82E-01	6.07E-02	2.86E-03
S5	5,000	M	6	2	1.55E+00	1.31E-01	2.64E-02	1.31E-03
S5	10,000	M	5	1	1.43E+00	1.01E-01	2.30E-02	1.01E-03
S5	1,200	U	8	1	4.57E-01	1.29E-03	8.64E-03	1.29E-05
S5	1,400	U	8	2	1.25E+01	2.74E-04	1.27E-01	2.78E-06
S5	3,000	U	6	3	1.66E+00	1.69E-01	3.13E-02	1.78E-03
S5	5,000	U	5	3	9.96E-01	7.85E-02	1.25E-02	7.92E-04
S5	10,000	U	5	1	9.05E-01	6.23E-02	1.37E-02	6.23E-04

Note: Volume releases less than $1 \times 10^{-7} \text{ m}^3$ have been reduced to 0.0 for the purposes of this table and the average DBR volume is calculated by the total of the DBR volumes divided by the total number of vectors. The DBR volume was obtained from the output variable BRIN_REL which is calculated in the ALGEBRACDB step 3 post processing step, see section 5.2.4.1, and contained in the ALG3 CDB files.

As seen in Table 6-2 through Table 6-6, the number of vectors with non-zero DBR volumes increased from the CRA-2004 PABC to the CRA-2009 PA. The greatest increase is seen in the middle and upper drilling locations for all scenarios and in the lower drilling location for scenarios S1, S4 and S5. The increase is similar between the middle and upper drilling locations.

Of the differences between the CRA-2009 PA and the CRA-2004 PABC DBR calculations listed in Section 4.3, many do not affect the number of non-zero DBR volumes. As discussed in Kirkes and Clayton (2008), the reduction of the maximum DBR duration parameter had no effect on the number of non-zero DBR volumes. As discussed in Section 4.3.2, the modified capillary pressure and relative permeability model do not affect the DBR calculations. The updates to permeability calculations do not affect the DBR calculations (see Section 4.3.3). The update to the well productivity index calculation only affects the upper drilling location DBR calculations (see Section 4.3.3), but as the increase in the non-zero DBR volumes is similar between the middle and upper drilling locations, the effect is therefore minimal. The updated computer codes do not affect the DBR calculations (Nemer 2007e) and Clayton (2007) shows that the input file corrections did not change the number of non-zero DBR volumes. Although many changes had no impact, they do improve the overall robustness of the computational methodology.

The increase in the number of non-zero DBR volumes is mainly due to the correction of the halite/disturbed rock zone porosity. Nemer and Clayton (2008) show that the repository pressure is positively correlated to the halite porosity, which is directly related to the disturbed rock zone porosity. Increasing the overall pressure increases the number of vectors with pressures above the 8 MPa threshold and can increase the DBR volume calculated to above zero. Furthermore, the increase in the halite/disturbed rock zone porosity increases the amount of brine available for transport into the repository, which can increase the repository saturation above the waste residual saturation threshold and increase the DBR volume calculated to above zero.

The maximum DBR volume increased in the S1, S4 and S5 scenarios for all three drilling locations and in the S2 and S3 scenarios for the middle and upper drilling locations for the CRA-2009 PA compared with the CRA-2004 PABC (Table 6-2 through Table 6-6). The maximum DBR volume generally decreased in the S2 and S3 scenarios for the lower drilling location for the CRA-2009 PA compared with the CRA-2004 PABC. For the CRA-2009 PA, the lower drilling location had a larger maximum DBR volume compared with the same scenario-time combination at the middle drilling location with a further decrease for the upper drilling location. This trend was also observed in the CRA-2004 PABC DBR results.

Table 6-2 through Table 6-6 shows that the CRA-2009 PA average DBR volume increased in the S1, S4 and S5 scenarios for all three drilling locations and in the S2 and S3 scenario for the middle and upper drilling locations compared with the CRA-2004 PABC values. The average DBR volumes are similar for the S2 scenario, lower drilling location for the two analyses. The average DBR volumes decreased for the S3 scenario, lower drilling location for the CRA-2009 PA compared with the CRA-2004 PABC.

Of the differences between the CRA-2009 PA and the CRA-2004 PABC DBR calculations listed in Section 4.3, many do not affect or have a minimal effect on the DBR volume calculation. The modified capillary pressure and relative permeability model do not affect the DBR calculations (see Section 4.3.2). As discussed in Section 4.3.3, the update to the equivalent permeability calculations do not affect the calculated DBR volume, as the equivalent

permeabilities are low enough that essentially that there is no significant flow in the 4.5 day period. Furthermore, the updates to the well productivity index calculation do not affect the lower and middle drilling location calculated DBR volumes. As the increase in the maximum and average DBR volumes for the middle and upper drilling locations is similar, it appears that the effect of updating the upper drilling location well productivity index calculation is minimal. The updated computer codes do not affect the DBR calculations (Nemer 2007e). Clayton (2007) shows that the input file corrections increased the maximum DBR volume by at most 5% and increased the average DBR volume by at most 3%. The reduction of the maximum DBR duration parameter decreased the maximum DBR volume for scenarios S2 and S3 by ~40%, with no change for S1, S4 and S5 and the average DBR volume decreased ~15% for all scenarios (Kirkes and Clayton 2008).

The correction of the halite/disturbed rock zone porosity increased the maximum and average DBR volumes in all scenarios. As the other changes had little or no effect and decreased the maximum and average DBR volumes, the effect of the increased halite/disturbed rock zone porosity appears to be to increase the maximum and average DBR volumes. Repository pressure is shown to be positively correlated to the halite porosity (Nemer and Clayton 2008), which is directly related to the disturbed rock zone porosity. Increasing the overall pressure increases pressure above the 8 MPa threshold and can increase the DBR volume calculated. Furthermore, the increase in the halite/disturbed rock zone porosity increases the amount of brine available for transport into the repository, which can increase the repository saturation above the waste residual saturation threshold and increase the DBR volume calculated.

To illustrate the effect on the DBR calculations as a result of the correction to the halite/disturbed rock zone porosity, scatter plots of disturbed rock zone porosity versus DBR volume for the S2 scenario, middle and upper drilling intrusion locations for the CRA-2009 PA and the CRA-2004 PABC are shown in Figure 3 and Figure 4, respectively. The middle and upper drilling locations were used as these locations are not confounded by the previous E1 intrusion. Calculations that resulted in effectively zero DBR volumes are shown as 10^{-7} m^3 for reference.

As seen in Figure 3 and Figure 4, the higher DBR volumes correspond to higher values of porosity. For the CRA-2009 PA, there are many more vectors with porosities above 0.03 compared with the CRA-2004 PABC, which then results in more vectors with non-zero DBR volumes and higher maximum and average DBR volumes.

A useful method of presenting DBR results is through the use of probability plots. A probability plot displays the percentage of the vectors on the X-axis where DBR volumes are less than the value on the Y-axis. The probability axis is scaled so that a normally distributed variable will plot as a straight line. This option was selected for these plots so that low probability DBRs are more visible.

Figure 5 to Figure 14 show probability plots for the lower drilling locations, S1-S5 for the CRA-2009 PA and the CRA-2004 PABC. For the CRA-2009 PA, the largest DBR volume and the greatest probability of a non-zero volume both occur in the S2 scenario, similar to the CRA-2004 PABC. No significant differences between the CRA-2009 PA and CRA-2004 PABC probability plots are observed.

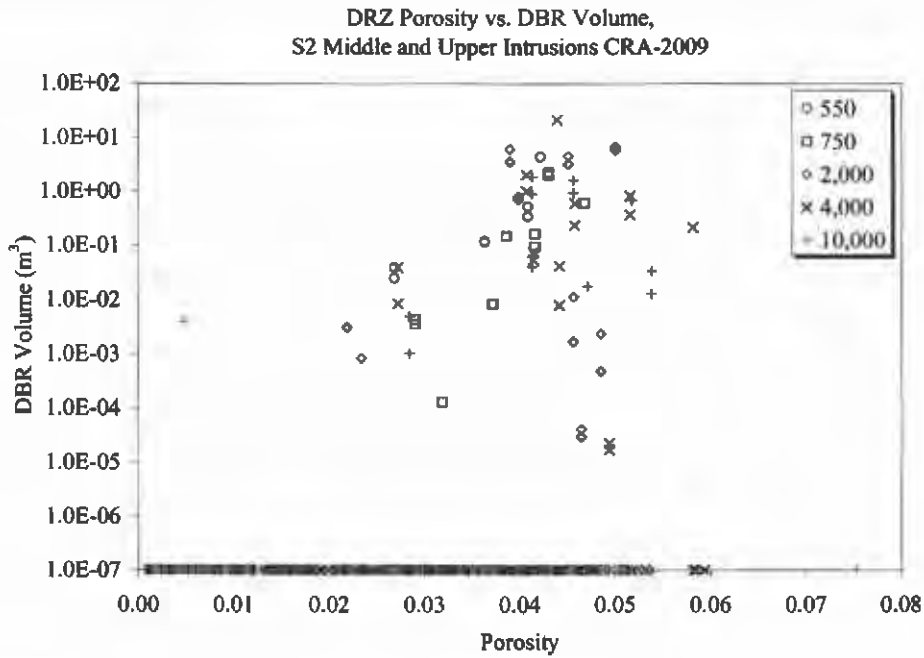


Figure 3. Scatter plot of pressure in the disturbed rock zone porosity vs. DBR volumes for the S2 scenario, lower drilling intrusion, CRA-2009 PA. Symbols indicate intrusion times in years.

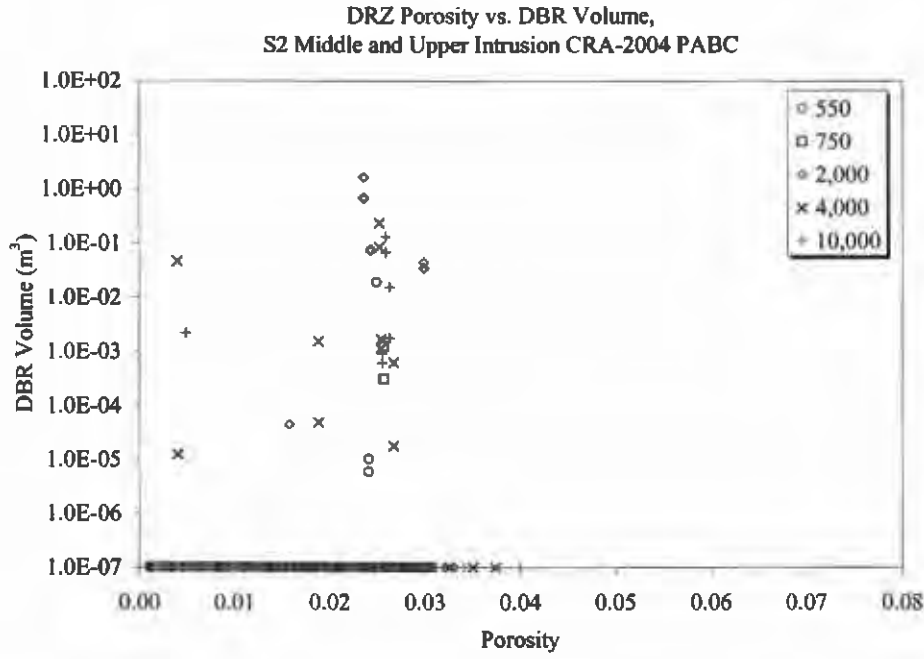


Figure 4. Scatter plot of pressure in the disturbed rock zone porosity vs. DBR volumes for the S2 scenario, lower drilling intrusion, CRA-2004 PABC. Symbols indicate intrusion times in years.

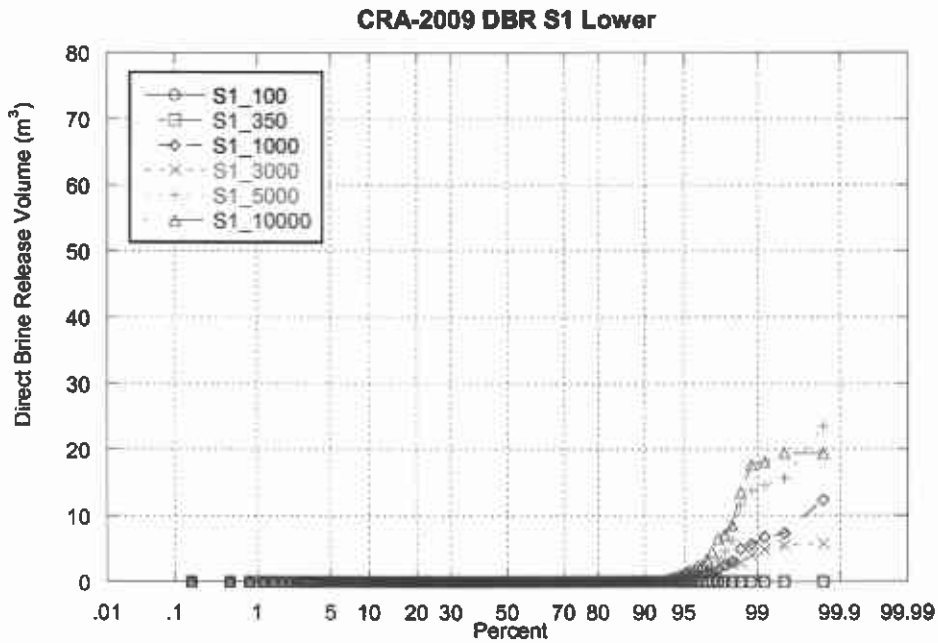


Figure 5. Probability plot showing the percentage of the vectors on the X-axis where DBR volumes are less than the value on the Y-axis for the CRA-2009 PA lower drilling location; S1 scenario.

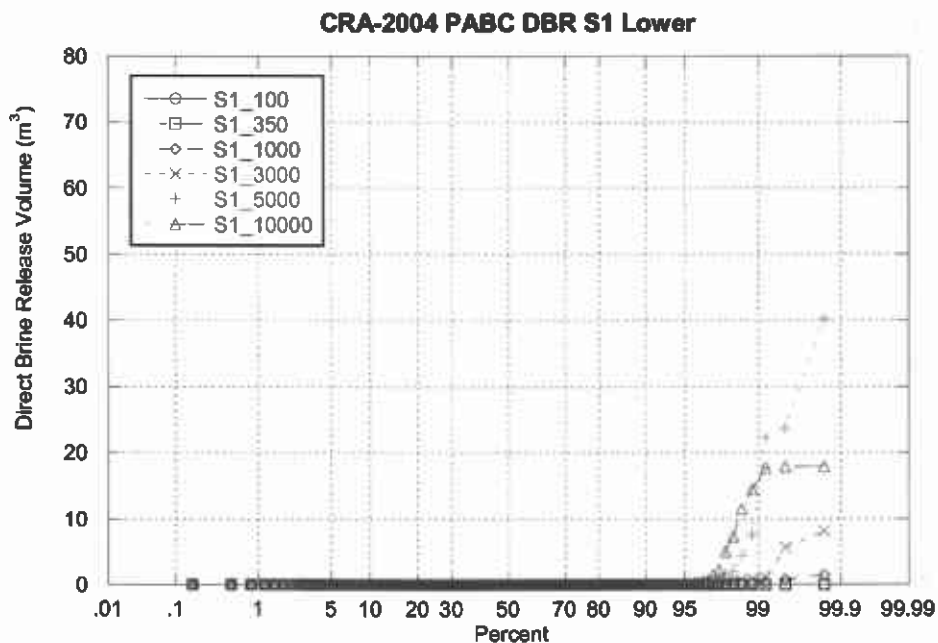


Figure 6. Probability plot showing the percentage of the vectors on the X-axis where DBR volumes are less than the value on the Y-axis for the CRA-2004 PABC lower drilling location; S1 scenario.

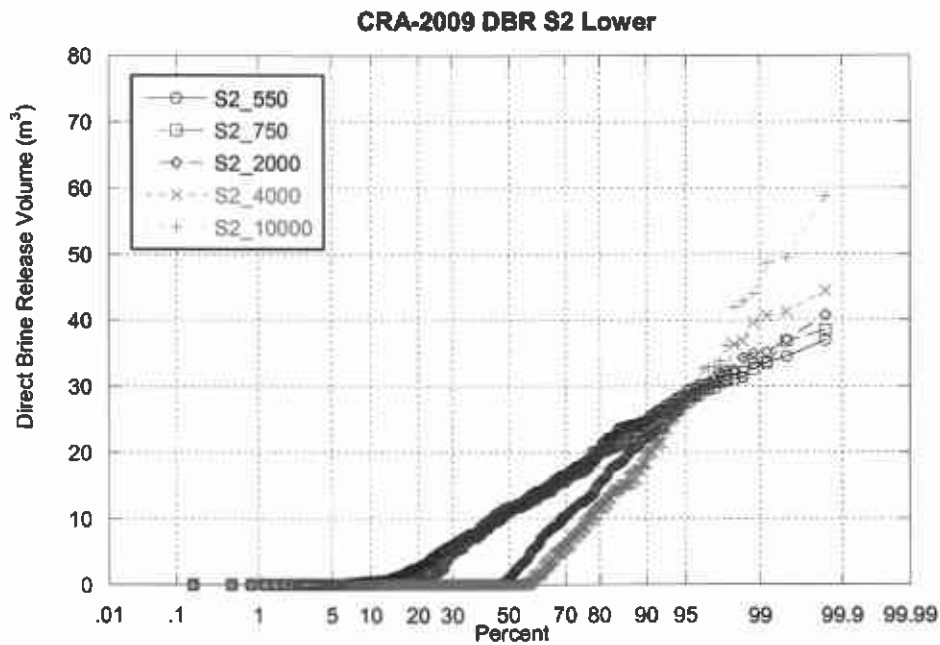


Figure 7. Probability plot showing the percentage of the vectors on the X-axis where DBR volumes are less than the value on the Y-axis for the CRA-2009 PA lower drilling location; S2 scenario.

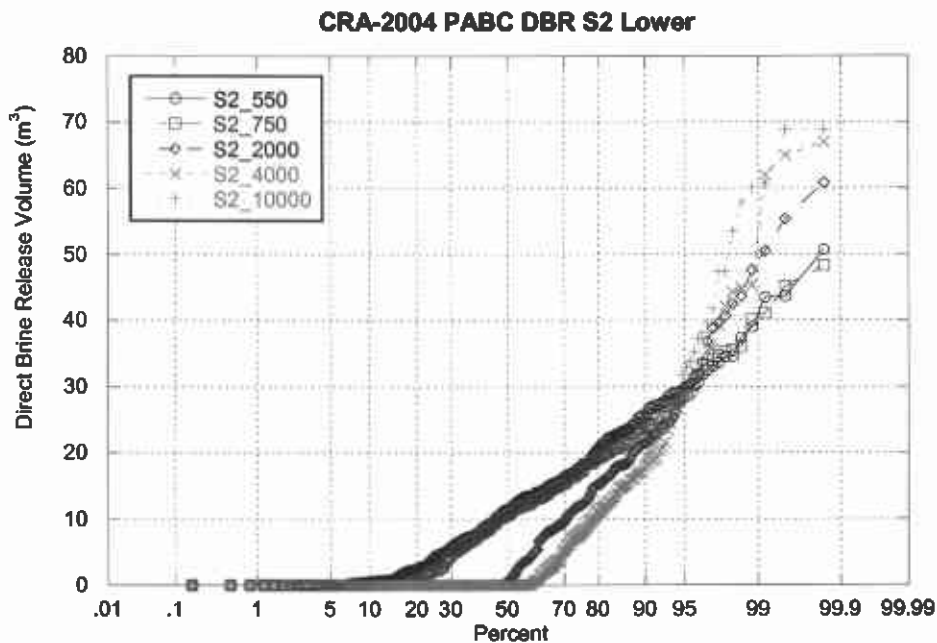


Figure 8. Probability plot showing the percentage of the vectors on the X-axis where DBR volumes are less than the value on the Y-axis for the CRA-2004 PABC lower drilling location; S2 scenario.

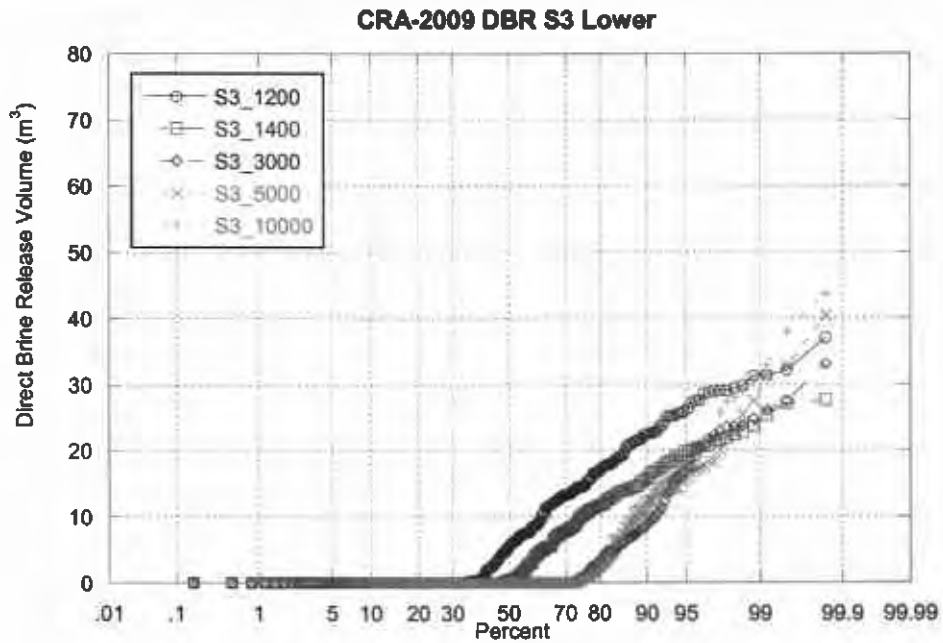


Figure 9. Probability plot showing the percentage of the vectors on the X-axis where DBR volumes are less than the value on the Y-axis for the CRA-2009 PA lower drilling location; S3 scenario.

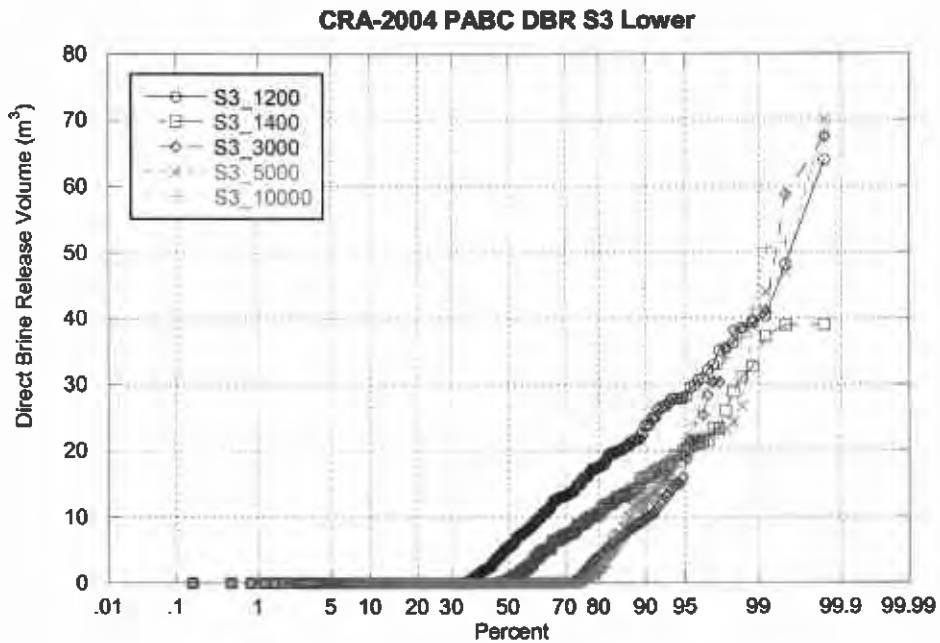


Figure 10. Probability plot showing the percentage of the vectors on the X-axis where DBR volumes are less than the value on the Y-axis for the CRA-2004 PABC lower drilling location; S3 scenario.

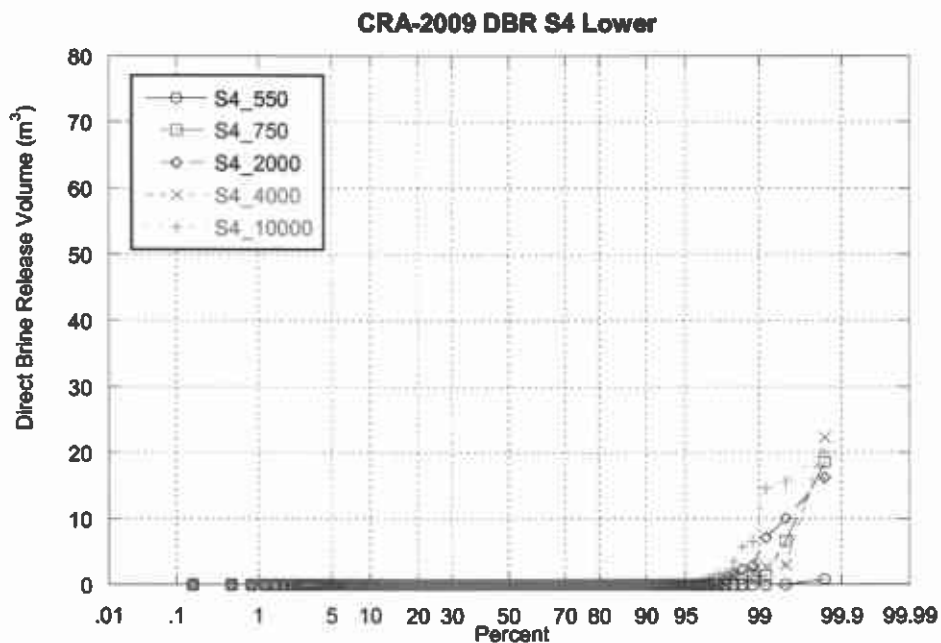


Figure 11. Probability plot showing the percentage of the vectors on the X-axis where DBR volumes are less than the value on the Y-axis for the CRA-2009 PA lower drilling location; S4 scenario.

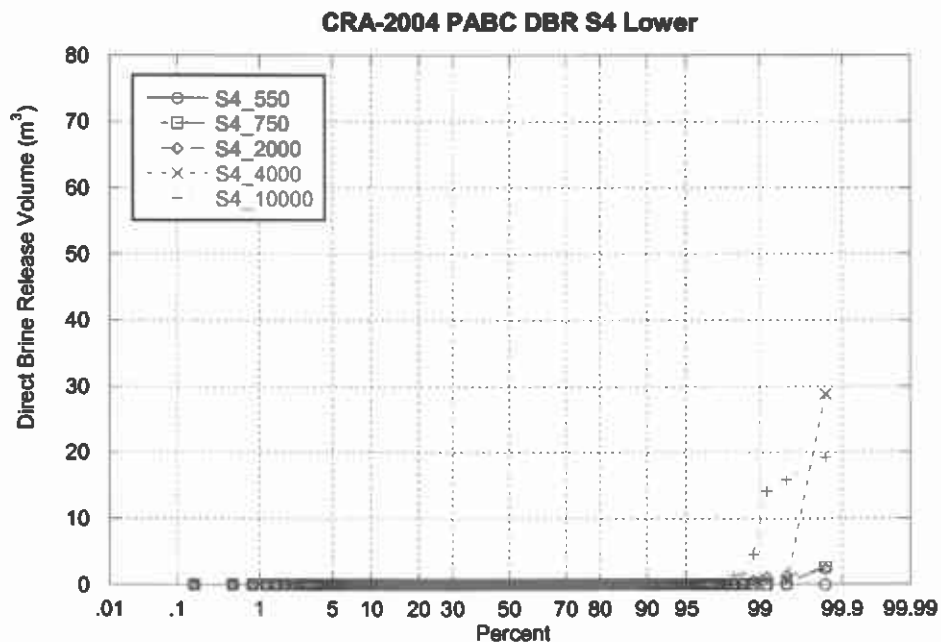


Figure 12. Probability plot showing the percentage of the vectors on the X-axis where DBR volumes are less than the value on the Y-axis for the CRA-2004 PABC lower drilling location; S4 scenario.

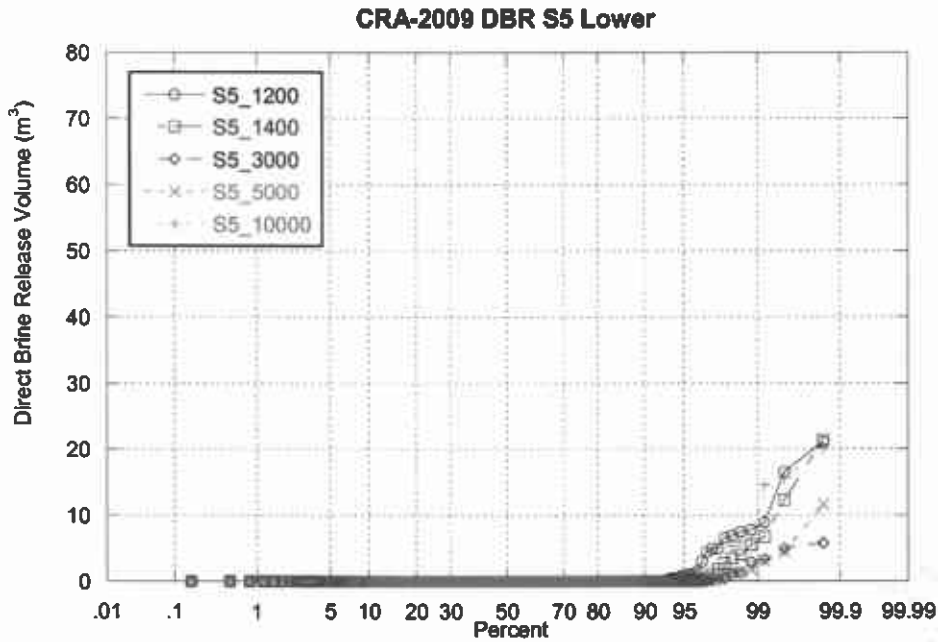


Figure 13. Probability plot showing the percentage of the vectors on the X-axis where DBR volumes are less than the value on the Y-axis for the CRA-2009 PA lower drilling location; S5 scenario.

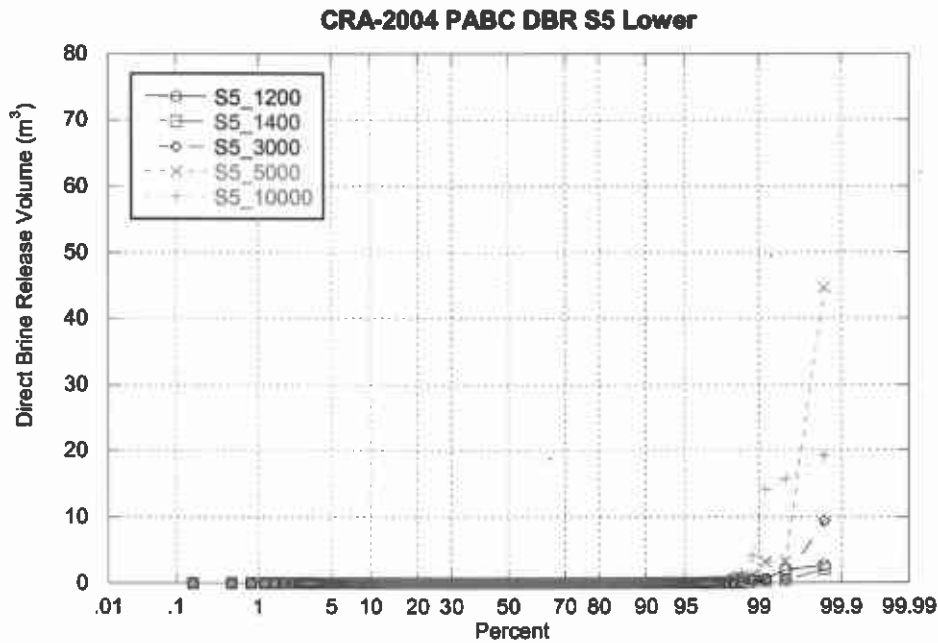


Figure 14. Probability plot showing the percentage of the vectors on the X-axis where DBR volumes are less than the value on the Y-axis for the CRA-2004 PABC lower drilling location; S5 scenario.

6.3 Sensitivity of Direct Brine Releases to Input Parameters

Sensitivity analyses for the CCA determined that waste pressure, brine saturation, and borehole permeability were the three most important variables that controlled DBR volumes (Helton et al. 1998). These three parameters continue to be the most important for DBR volumes in the CRA-2009 PA. For the plots given below, the values of these parameters were extracted from the ALG2 files from the DBR calculations. A more detailed description of these files is contained in Section 5.2.2.5.

Scenarios S2 and S3 have significant DBR volumes because of the presence of a previous borehole connecting the repository with the Castile brine reservoir, which generally increases the waste panel pressure. The sensitivity analysis will focus on the S2 and S3 scenarios because these scenarios have the greatest number of significant DBR volumes. Scenarios S1, S4, and S5 have so few runs with non-zero DBR volumes that these scenarios are excluded from the sensitivity analysis. As scenarios S2 and S3 are similar, only scenario S2 is used in the sensitivity analysis.

Pressure in the intruded panel at the time of the intrusion is an important factor for many vectors. Figure 15 and Figure 16 and show scatter plots of pressure in the intruded panel versus DBR volume for the S2 scenario, lower drilling intrusion for the CRA-2009 PA and the CRA-2004 PABC, respectively. These figures clearly show that there are no DBRs until pressures exceed 8 MPa as indicated by the vertical line in the figures. Above 8 MPa, a significant number of vectors have zero volumes; these vectors have mobile brine saturations (brine saturation minus residual brine saturation) less than zero and thus no brine is available in a mobile form to be released. Figure 17 and Figure 18 show that DBR volumes tend to increase with increasing pressure and increasing mobile saturation.

Figure 15 and Figure 16 show a high concentration of results that are near a line extending from 0 m³ and 8 MPa to 30 m³ and 12 MPa. This correlation does not appear to vary with time as values from the five different times are all present in this area. Figure 17 and Figure 18 show that as mobile saturation increases, the correlation between pressure and DBR volumes also increases. There is a great deal of similarity between the sensitivity results of the CRA-2009 PA and the CRA-2004 PABC with regard to pressure and mobile brine saturation. One point to note is that the highest mobile saturations do not correspond to the highest DBR volumes in either calculation. This is because pressure and saturation tend to be inversely correlated for high pressures in the 10,000 year BRAGFLO results (Nemer and Clayton 2008).

Figure 19 and Figure 20 plot pressure versus mobile brine saturation for the S2 scenario for all intrusion times with symbols indicating the range of DBR volumes, for the CRA-2009 PA and CRA-2004 PABC, respectively. It is clear from these figures that not all the variability in DBR volumes can be explained by pressure and saturation alone.

Figure 21 and Figure 22 show scatter plots of the log of borehole permeability vs. DBR volumes for the S2 scenario, lower drilling intrusion with symbols indicating intrusion times for the CRA-2009 PA and CRA-2004 PABC, respectively. The sensitivity of the DBR volume to the borehole permeability decreased in the CRA-2009 PA results. Similar DBR volumes exist for the entire range of borehole permeability for the CRA-2009 PA results (Figure 21), while for the CRA-2004 PABC, the higher volumes tend toward the lower permeability range (Figure 22).

Borehole permeability is used in the boundary condition well calculations. This parameter also affects conditions in the repository as modeled in the 10,000-year BRAGFLO calculations, which are used as initial conditions of the DBR model. As borehole permeability increases DBR volumes tend to decrease, especially at late intrusion times (4,000 and 10,000 years). Helton et al. (1998) identified this same relationship for the CCA results. Since the lower drilling intrusion disturbed scenarios represent the second or subsequent intrusion into the same panel of the repository and the borehole permeability is sampled only once per vector, low borehole permeability tends to result in higher pressures following the first intrusion. This occurs because low borehole permeability does not allow the panel to depressurize during the first intrusion to the extent as occurs when the borehole is highly permeable. High pressures following a previous intrusion tend to result in higher DBR volumes during the subsequent intrusion.

6.4 Conclusions

The DBR results from replicate 1 of the CRA-2009 PA and CRA-2004 PABC show that DBRs to the surface are very unlikely for most intrusions into the repository and in most cases result in inconsequential DBR volumes. The exception to this statement is for intrusions into a panel that had previously experienced a brine reservoir intrusion. Such intrusions are represented in PA by the lower drilling intrusions in the S2 and S3 scenarios. During these events, the results of the CRA-2004 PABC predict that it is possible that as much as 59 m³ of contaminated brine from the repository can reach the surface; however, in most cases the volume is much less. The correction of the halite/disturbed rock zone porosity increased the number of non-zero, maximum and average DBR volumes for the CRA-2009 PA compared with the CRA-2004 PABC, especially for the middle and upper drilling locations. The changes incorporated into the DBR calculations will not adversely affect overall releases.

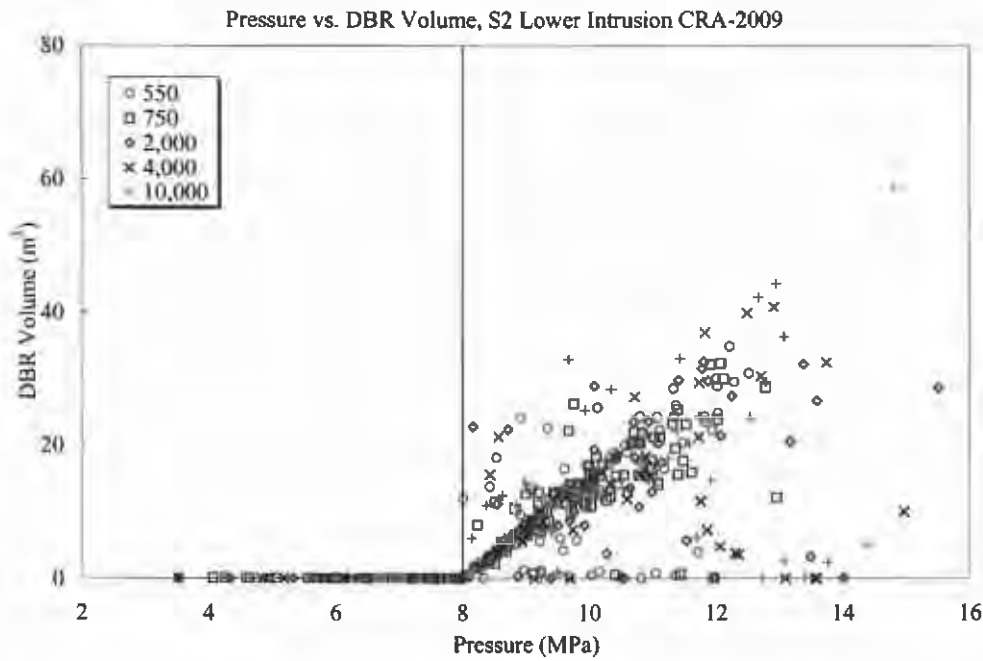


Figure 15. Scatter plot of pressure in the intruded panel vs. DBR volumes for the S2 scenario, lower drilling intrusion, CRA-2009 PA. Symbols indicate intrusion times in years.

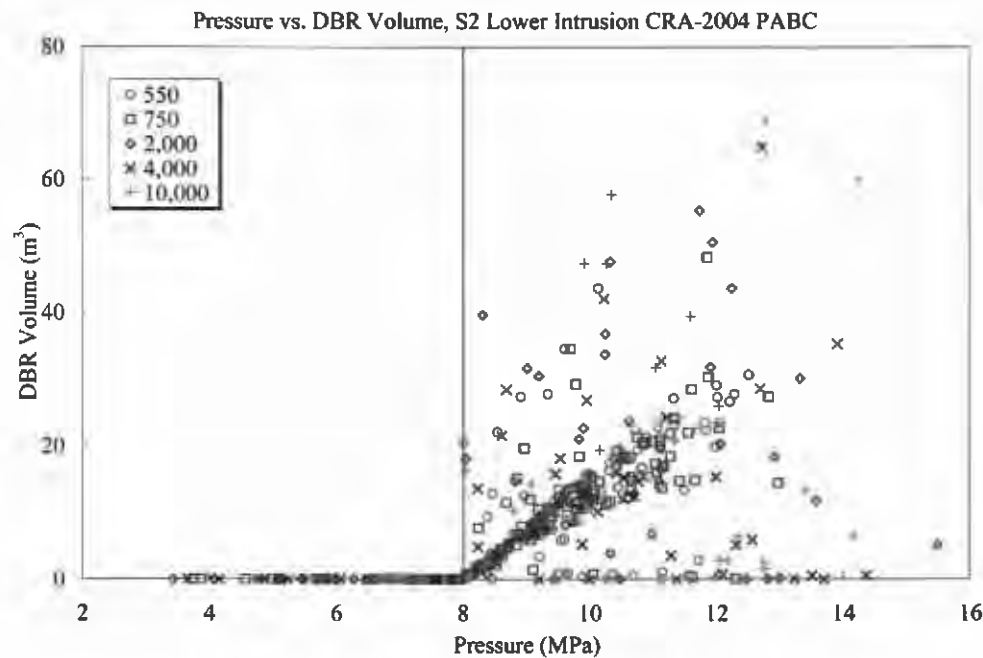


Figure 16. Scatter plot of pressure in the intruded panel vs. DBR volumes for the S2 scenario, lower drilling intrusion, CRA-2004 PABC. Symbols indicate intrusion times in years.

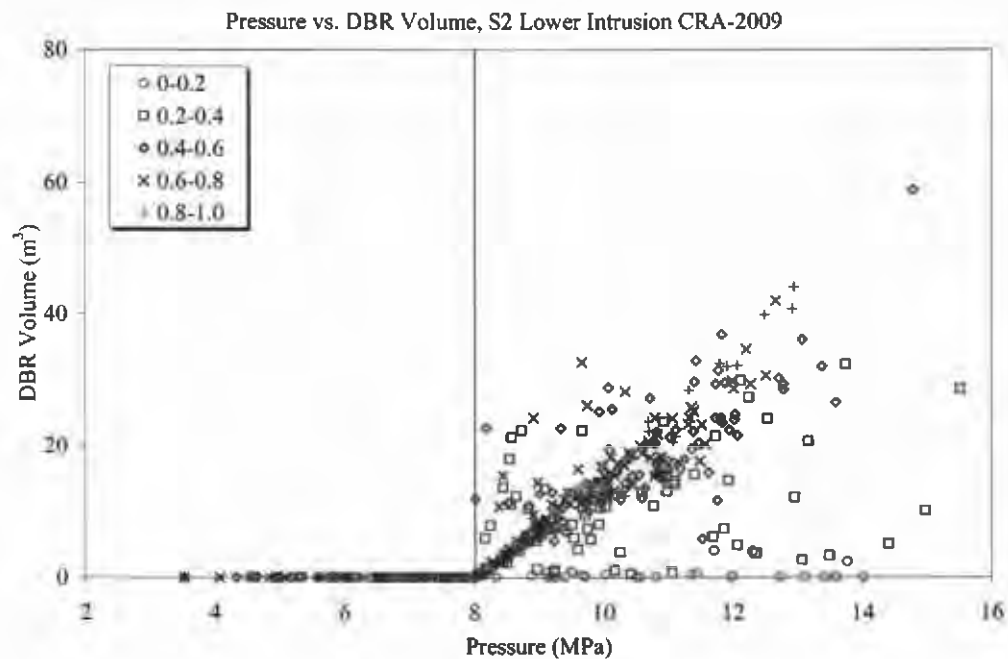


Figure 17. Scatter plot of pressure in the intruded panel vs. DBR volumes for the S2 scenario, lower drilling intrusion, CRA-2009 PA. Symbols indicate the range of mobile brine saturation.

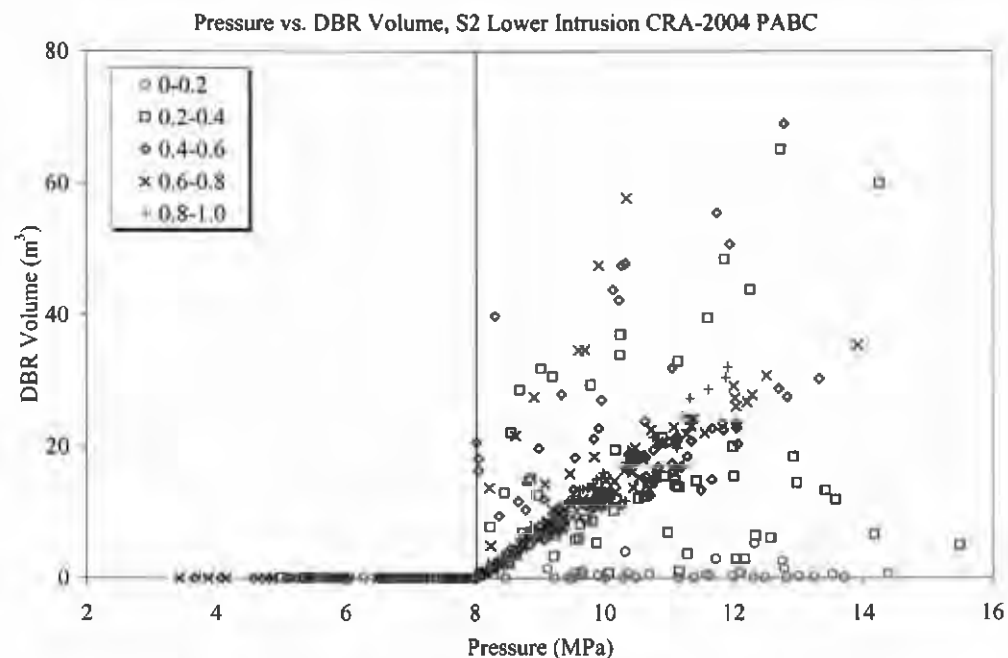


Figure 18. Scatter plot of pressure in the intruded panel vs. DBR volumes for the S2 scenario, lower drilling intrusion, CRA-2004 PABC. Symbols indicate the range of mobile brine saturation.

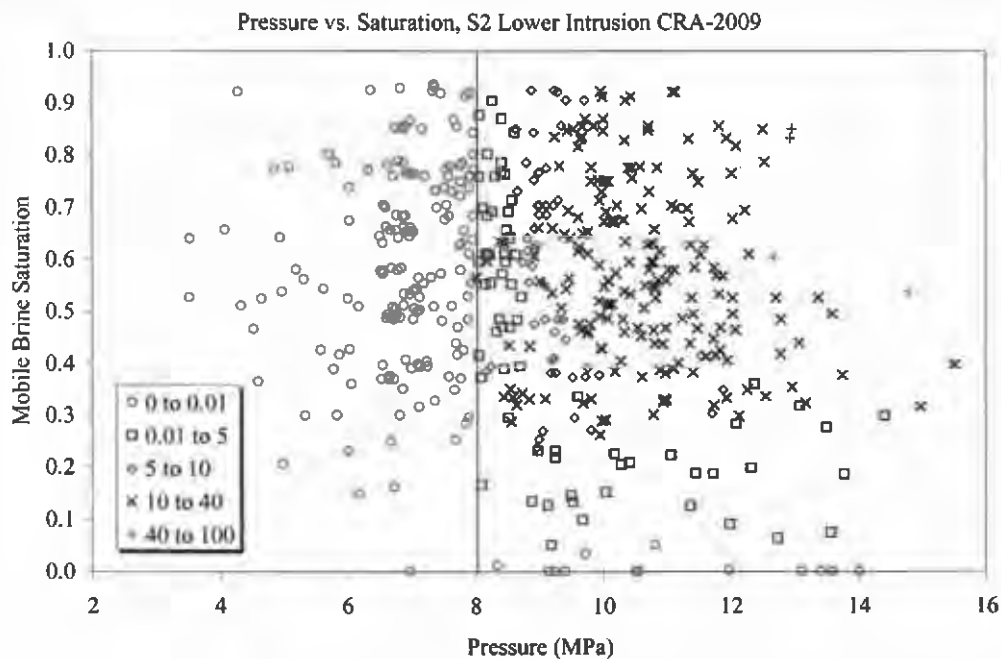


Figure 19. Scatter plot of pressure vs. mobile brine saturation for the S2 scenario, lower drilling intrusion, all intrusion times, CRA-2009 PA. Symbols indicate the range of DBR volumes in m^3 .

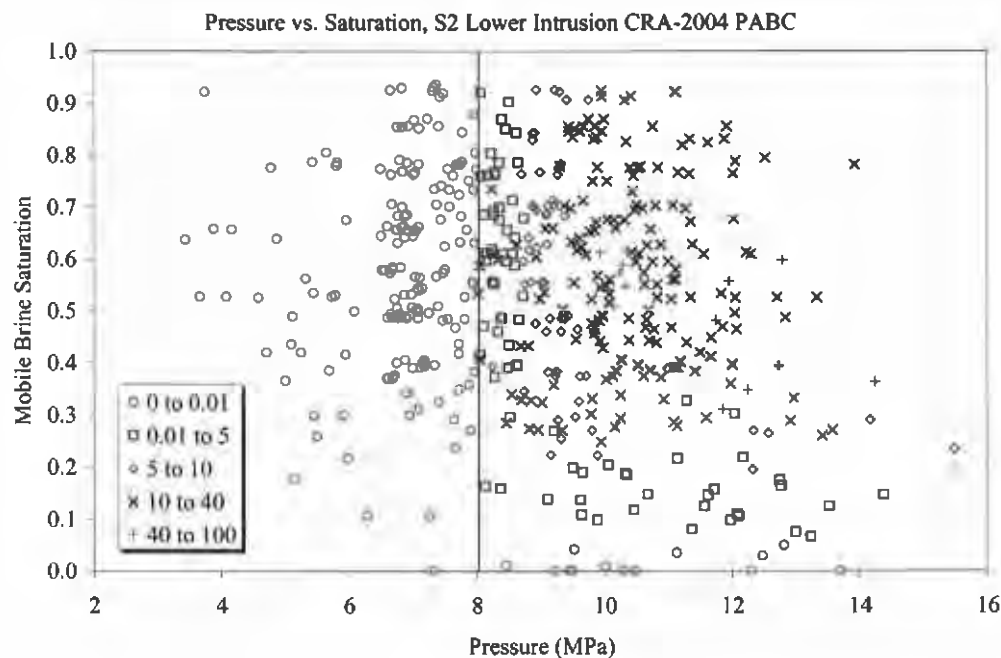


Figure 20. Scatter plot of pressure vs. mobile brine saturation for the S2 scenario, lower drilling intrusion, all intrusion times, CRA-2004 PABC. Symbols indicate the range of DBR volumes in m^3 .

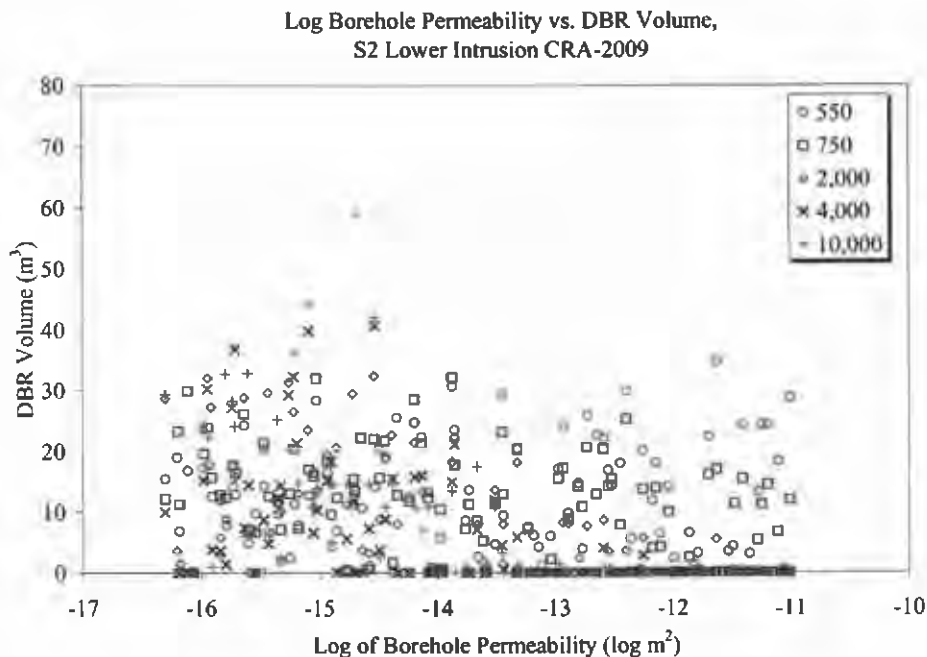


Figure 21. Scatter plot of the log of borehole permeability vs. DBR volumes for the S2 scenario, lower drilling intrusion, CRA-2009 PA. Symbols indicate the intrusion time in years.

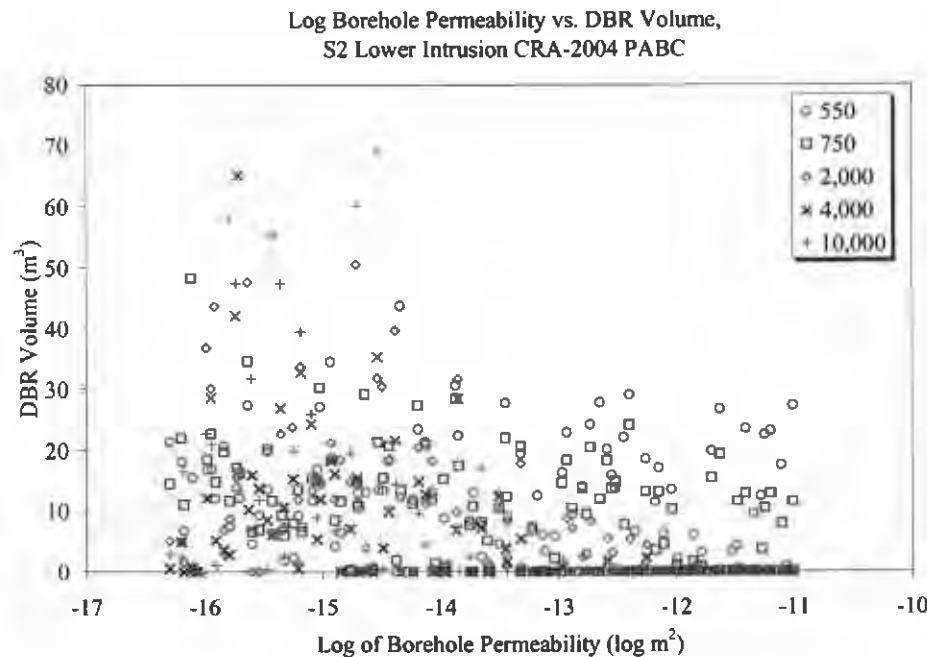


Figure 22. Scatter plot of the log of borehole permeability vs. DBR volumes for the S2 scenario, lower drilling intrusion, CRA-2004 PABC. Symbols indicate the intrusion time in years.

7 SOFTWARE LIST

The major codes that were used for the CRA-2009 PA DBR calculations are listed in Table 7-1. Calculations were performed on qualified ES45 and ES47 Compaq ALPHA computers running Open VMS Version 8.2.

Table 7-1. Codes that were used in the CRA-2009 PA DBR calculations.

Code	Version	Code Function
ALGEBRACDB	2.35	Data processor
BRAGFLO	6.00	Brine and gas flow
GENMESH	6.08	Grid generation
ICSET	2.22	Sets initial conditions
MATSET	9.10	Sets material parameters
POSTBRAG	4.00A	BRAGFLO postprocessor
PREBRAG	8.00	BRAGFLO preprocessor
RELATE	1.43	Grid data processor
SUMMARIZE	2.20	Data interpolation

8 REFERENCES

- Brooks, R.H. and A.T. Corey. (1964). Hydraulic Properties of Porous Media. Hydrology Paper No. 3. Fort Collins, CO: Colorado State University. ERMS 241117.
- Caporuscio, F., J. Gibbons and E. Oswald. (2003). Waste Isolation Pilot Plant: Salado Flow Conceptual Models Final Peer Review Report. U.S. Department of Energy, Carlsbad Area Office, Office of Regulatory Compliance, Carlsbad, NM. ERMS 526879.
- Chappelear, J.E. and A.S. Williamson (1981). Representing Wells in Numerical Reservoir Simulation. ERMS 249488.
- Clayton, D.J. (2007). Corrections to Input Files for DBR PABC Calculations. Sandia National Laboratories, Carlsbad, NM. ERMS 546311.
- Clayton, D.J. (2008). Analysis Plan for the Performance Assessment for the 2009 Compliance Recertification Application. Analysis Plan AP-137, Revision 1. Sandia National Laboratories, Carlsbad, NM. ERMS 547905.
- Cotsworth, E. (2005). EPA Letter on Conducting the Performance Assessment Baseline Change (PABC) Verification Test. U.S. EPA, Office of Radiation and Indoor Air, Washington, D.C. ERMS 538858.
- Garner, J.R. and C.D. Leigh (2005). Analysis Package for PANEL: CRA-2004 Performance Assessment Baseline Calculation. Sandia National Laboratory, Carlsbad, NM. ERMS 540572.
- Gilkey, A.P. (2007). Change Control for PREBRAG, Version 7.00, (Proposed 8.00). Sandia National Laboratories, Carlsbad, NM. ERMS 545263.
- Hadgu, T. (2002). Analysis Plan for the Analysis of Direct Releases Part of the Technical Baseline Migration. Sandia National Laboratories, Carlsbad, NM. ERMS 522634.
- Hadgu, T., P. Vaughn, J.E. Bean, D. Johnson, J. Johnson, K. Aragon and J. Helton. (1999). Modifications to the 96 CCA direct brine release calculations. Sandia National Laboratories, Carlsbad, NM. ERMS 511276.
- Hansen, C.W. (2003). Design Document/User's Manual for CCDFGF Version 5.00. Sandia National Laboratories, Carlsbad, NM. ERMS 530471.
- Helton, J.C, J.E. Bean, F.W. Berglund, F.J. Davis, K. Economy, J.W. Garner, J.D. Johnson, R.J. MacKinnon, J. Miller, D.G. O'Brien, J.L. Ramsey, J.D. Schreiber, A. Shinta, L.N. Smith, D.M. Stoelzel, C. Stockman and P. Vaughn. (1998). Uncertainty and Sensitivity Analysis Results Obtained in the 1996 Performance Assessment for the Waste Isolation Pilot Plant. Sandia National Laboratories, Albuquerque, NM. SAND98-0365, ERMS 252619.
- Ismail, A.E. (2007a). Parameter Problem Report (PPR), PPR-2007-002 for S_HALITE, DRZ_0. Sandia National Laboratories, Carlsbad, NM. ERMS 545713.
- Ismail, A.E. (2007b). Revised Porosity Estimates for the DRZ. Sandia National Laboratories, Carlsbad, NM. ERMS 545755.

-
- Ismail, A.E. (2008). Analysis Package for CUTTINGS_S: Compliance Recertification Application 2009, Revision 1. Sandia National Laboratories. Carlsbad, NM.
- Kirkes, G.R. (2007). Evaluation of the Duration of Direct Brine Release in WIPP Performance Assessment. April 27, 2007. Sandia National Laboratories, Carlsbad, NM. ERMS 545988.
- Kirkes, G.R. and C.G. Herrick. (2006). Analysis Plan for the Modification of the Waste Shear Strength Parameter and Direct Brine Release Parameters. AP-131. Sandia National Laboratories, Carlsbad, NM. ERMS 545130.
- Kirkes, G.R. and D.J. Clayton. (2008). Impact Analysis of Decreased Duration of Direct Brine Release in WIPP Performance Assessment. Sandia National Laboratories, Carlsbad, NM. ERMS 548313.
- Lee, J. 1982. Well Testing. SPE Textbook Series Vol. 1. New York, NY: Society of Petroleum Engineers of AIME.
- Leigh, C.D., J.F. Kanney, L.H. Brush, J.W. Garner, G.R. Kirkes, T. Lowry, M.B. Nemer, J.S. Stein, E.D. Vugrin, S. Wagner, and T.B. Kirchner. (2005). 2004 Compliance Recertification Application Performance Assessment Baseline Calculation, Revision 0. Sandia National Laboratories, Carlsbad, NM. ERMS 541521.
- Long, J.J. (2008). Execution of Performance Assessment Codes for the 2009 Compliance Recertification Application Performance Assessment, Revision 0. Sandia National Laboratories. Carlsbad, NM. ERMS 548350.
- Mattax, C.C. and R.L. Dalton. (1990). Reservoir Simulation. Henry L. Doherty Memorial Fund Society of Petroleum Engineers Inc., Richardson, TX.
- Nemer, M.B. (2007a). Change Control for POSTBRAG, Version 4.00, (Proposed 4.00A). Sandia National Laboratories, Carlsbad, NM. ERMS 545687.
- Nemer, M.B. (2007b). Design Document for BRAGFLO Version 6.0. Sandia National Laboratories, Carlsbad, NM. ERMS 545015.
- Nemer, M.B. (2007c). Software Problem Report (SPR) 07-001 for POSTBRAG, Version 4.00. Sandia National Laboratories, Carlsbad, NM. ERMS 545686.
- Nemer, M.B. (2007d). User's Manual for BRAGFLO Version 6.0. Sandia National Laboratories, Carlsbad, NM. ERMS 545016.
- Nemer, M.B. (2007e). Validation Document for BRAGFLO Version 6.0. Sandia National Laboratories, Carlsbad, NM. ERMS 545018.
- Nemer, M.B. and D.J. Clayton. (2008). Analysis Package for BRAGFLO: Compliance Recertification Application 2009. Sandia National Laboratories. Carlsbad, NM.
- SNL (1997). Final, Supplemental Summary of EPA-Mandated Performance Assessment Verification Test (All Replicates) and Comparison with the Compliance Certification Application Calculations. Sandia National Laboratories. Carlsbad, NM. ERMS 414879.

-
- Stein, J.S., M.B. Nemer and J.R. Trone. (2005) Analysis Package for Direct Brine Releases: Compliance Recertification Application – 2004 PABC. Sandia National Laboratories. Carlsbad, NM. ERMS 540633.
- Stoelzel, D.M. and D.G. O'Brien (1996). Conceptual Model Description of BRAGFLO Direct Brine Release Calculations to Support the Compliance Certification Application (CCA MASS Attachment 16-2). U.S. Department of Energy, Carlsbad, NM. ERMS 239090.
- U. S. Congress (1992). Waste Isolation Pilot Plant Land Withdrawl Act. Public Law 102-579, as amended by Public Law 104-201. September 1996. 104th Congress, Washington D.C.
- U. S. DOE (1980). Final Environmental Impact Statement: Waste Isolation Pilot Plant. U.S. Department of Energy, Assistant Secretary for Defense Programs, Vols. 1-2., Washington, D.C. DOE/EIS-0026, ERMS 238839.
- U. S. DOE (1990). Final Supplement: Environmental Impact Statement, Waste Isolation Pilot Plant. U.S. Department of Energy, Office of Environmental Restoration and Waste Management. Vols. 1-13, Washington, D.C. DOE/EIS-0026-FS, ERMS 247955 and 243022.
- U. S. DOE (1993). Waste Isolation Pilot Plant Strategic Plan. U.S. Department of Energy, Washington, D.C. ERMS 251353.
- U.S. DOE (1996). Title 40 CFR Part 191 Compliance Certification Application for the Waste Isolation Pilot. U.S. Department of Energy Waste Isolation Pilot Plant, Carlsbad Area Office, Carlsbad, NM. DOE/CAO-1996-2184.
- U.S. EPA (1996). 40 CFR 194. Criteria for the Certification and Recertification of the Waste Isolation Pilot Plant's Compliance with the 40 CFR Part 191 Disposal Regulations; Final Rule. U.S. Environmental Protection Agency, Washington, DC. ERMS 241579.
- van Genuchten, R. (1978). Calculating the Unsaturated Hydraulic Conductivity with a New Closed-Form Analytical Model. Research Report 78-WR-08. Princeton, NJ: Princeton University, Department of Civil Engineering. ERMS 249486.